International
Progress Report

IPR-02-66

Äspö Hard Rock Laboratory

Determination of the coefficient of therminal expansion for two Äspö rocks, Diorite and Granite

Kristina Larsson

University of Luleå

April 2001

Svensk Kärnbränslehantering AB
Swedish Nuclear Fuel
and Waste Management Co
Box 5864
SE-102 40 Stockholm Sweden
Tel +46 8 459 84 00
Fax +46 8 661 57 19

Äspö Hard Rock
Laboratory

Report no.
IPR-02-66
No.
F100K
Author
Larsson
Date
01-05-01
Checked by
Rolf Christiansson
Date
01-05-31
Approved
Christer Svemar
Date
02-12-05

Äspö Hard Rock Laboratory

Determination of the coefficient of therminal expansion for two Äspö rocks, Diorite and Granite

Kristina Larsson

University of Luleå

April 2001

Keywords: Thermal expansion, heat transport, Prototype Repository

Preface

The research presented in this study was carried out at the department of Rock Mechanics at Luleå University of Technology between April 2000 and February 2001.

The research work was made possible through financial support from the Swedish Nuclear Fuel and Waste Management Company (SKB).

I wish to express my thanks to my supervisor Erling Nordlund, LTU, for patiently reading, advising and commenting upon this work.

Luleå, April 2001

Kristina Larsson

Abstract

In the Prototype Repository at Äspö HRL (Hard Rock Laboratory) research is done to determine the rock mass response to storage of nuclear waste. Nuclear waste gives off heat, which will increase the temperature of the surrounding rock. The effects of heating the rock is studied by placing electrical heaters in the deposition holes to simulate the heat generated by the radioactive waste. Maximum temperature on the rock surface in the deposition holes will be about 70°C. This will produce thermomechanical loading and potential microcracking between the mineral grains due to differential thermal expansion. The microcracks affect the mechanical and hydrogeological properties of the rock mass, which may have an influence on the integrated function of the storage, such as the water saturation process and deformations. It is therefore important to know the amount of thermomechanical loading and potential microcracking that is likely to occur at a given temperature increase. This can be simulated when the coefficient of thermal expansion and the grain size of the rock types present at the site are known.

The aim of this study was to determine the coefficient of thermal expansion for two rock types from Äspö, diorite and granite. This was done by using strain gauges glued to the samples and measuring the axial and tangential strain as the temperature varied between room temperature and 70°C. The linear coefficient of thermal expansion (α) was then calculated by dividing the measured axial expansion with the temperature interval. The values of the linear coefficient achieved were compared to values found in the literature and were found to be within the same order of magnitude. The volumetric coefficient of expansion was calculated in two ways, first using the measured axial and tangential strains and then by using the common assumption that the value of the volumetric coefficient is three times the value of the axial coefficient. These two methods were then compared and were found to be in fair agreement with each other for both rock types. The samples were also tested under a load of about 4 MPa, to see if the load would influence the thermal expansion. The conclusion was that no significant difference could be seen between the unloaded and loaded condition. Six out of seven samples were tested immerged in water since the conditions at Äspö are saturated.

The coefficient of thermal expansion is influenced by several factors including heating rate, grain size of the samples and surrounding pressure. The heating rate was kept low since that reduces the amount of microcracking in the samples and also represents the actual conditions. The effect of differential thermal expansion between grains of different sizes in the sample can be minimized by applying the strain gauges across as many grains as possible. Doing this will give a more representative value of the expansion of the whole sample. A high surrounding pressure can prevent microcracking, but the major principle stress at the depth of sampling at Äspö is about 40 MPa, which is too low to influence the microcracking.

Sammanfattning

I studierna av bergmassan som omger prototypförvaringen i Äspölaboratoriet ingår som en del att ta reda på effekterna av att bergmassan värms upp som en följd av deponering av kärnbränsle. Detta sker genom placering av elektriska värmare i deponeringshålen för att simulera den värme som kommer att avges av det radioaktiva kärnbränslet. Maximal temperatur på deponeringshålens bergytor kommer att bli ca 70°C. Denna uppvärmning kommer att ge en termomekanisk belastning och möjligen mikrosprickor mellan mineralkornen på grund av differentiell värmeutvidgning. Mikrosprickor påverkar bergets mekaniska och hydrogeologiska egenskaper, vilka kan inverka på lagrets funktioner, som till exempel vattenmättnadsprocessen och deformationerna. Det är därför viktigt att känna till den termomekaniska belastningen samt den möjliga mikrouppsprickningens omfattning vid en given temperaturökning. Dessa kan simuleras om man känner till värmeutvidgningskoefficienten samt kornstorleken för de bergarter som finns närmast lagret.

Målet med denna rapport var att bestämma värmeutvidgningskoefficienten för två bergarter från Äspö, diorit och granit. Detta gjordes genom att limma töjningsgivare på provet och sedan mäta den axiella och tangentiella utvidgningen mellan rumstemperatur och 70°C. Den linjära värmeutvidgningskoefficienten (α) bestämdes sedan genom att dividera den uppmätta axiella töjningen med temperaturintervallet. De linjära α-värden var av samma storleksordning som annan forskning inom området uppvisat. Den volymetriska koefficienten bestämdes på två olika sätt, det första var att beräkna den utifrån uppmätta axiella och tangentiella töjningar och den andra att använda det vanligt förekommande antagandet att den volymetriska koefficienten är lika med tre gånger den axiella koefficienten. Dessa två metoder gav ungefär samma värde på den volymetriska koefficienten. Proverna testades också med en belastning på ca 4 MPa, för att se om detta på verkade värmeutvidgningskoefficienten. Inga tydliga skillnader kunde dock urskiljas mellan de obelastade och belastade proverna. Sex av sju prover testades i vatten eftersom förhållandena i Äspö är vattenmättade.

Värmeutvidgningskoefficienten påverkas av uppkomsten av mikrosprickor, som i sin tur påverkas av flera olika faktorer som t. ex upphettningshastighet och omgivande tryck. Effekten av differentiell värmeutvidgning mellan olika mineral av olika kornstorlek kan minimeras genom att applicera töjningsgivarna över så många korn som möjligt. Man får då ett värde på utvidgningen som är representativt för hela provet. Upphettningshastigheten hölls låg för att undvika uppkomst av mikrosprickor och för att efterlikna verkliga förhållanden. Ett högt omgivande tryck kan förhindra att mikrouppsprickning sker, men största huvudspänningen på det djup proverna tagits från är ca 40 MPa, vilket är för lågt för att ha någon effekt på mikrouppsprickningen.

Table of contents

1 Introduction

1.1 Background

In the Prototype Repository at Äspö HRL (Hard Rock Laboratory) research is done to determine the rock mass response to storage of nuclear waste. Nuclear waste gives off heat, which will increase the temperature of the surrounding rock. The effect of heating the rock is studied by placing electrical heaters in the rock mass to simulate the heat generated by the radioactive waste. At present the plans are to simulate a decay heat of about 1800 W/canister. Maximum temperature on the rock surface in the deposition holes will be about 70°C. This will produce thermomechanical loading and microcracking between the mineral grains due to differential thermal expansion depending on the magnitude of the differential temperature (Wilkins et al., 1985a). The microcracking will vary with time and distance from the storage as the temperature varies. The microcracks affect the mechanical and hydrogeological properties of the rock mass, which may have an influence on the integrated function of the storage, such as the water saturation process and deformations. Microcracks may increase the rock mass permeability around the deposition holes and thereby influence the water saturation rate of the bentonite buffer surrounding the copper canisters. Further the microcracks and potential displacements of adjacent joints may increase the possibility of water circulating around the stored waste, which in turn increases the potential risk of water contaminated by radioactivity to reach the ground water and be transported great distances. To account for this it is important to know the amount of thermomechanical loading and potential microcracking that is likely to occur at a given temperature increase (Wilkins et al., 1985b). The coefficient of thermal expansion and the grain size are important parameters that are needed to simulate the amount of thermal microcracking that could occur due to the placement of nuclear waste.

1.2 Objective

The aim of this study is to determine the coefficient of both axial and volumetric thermal expansion for two rock types from Äspö, diorite and granite. The study is a part of a project aimed at increasing the understanding of the behavior of heated rock.

1.3 Scope and limitations

The scope of the laboratory work was to determine the coefficient of thermal expansion in the temperature interval 20º C to 70º C. This interval was decided because the estimated temperature of the rock surface in the deposition holes is about 70º C. Some samples were tested first without load and then with load, while others were tested only without load or with the load only. All samples but one were tested in water since the in situ conditions at Äspö are saturated. One of the granite samples was tested in air, in order to see if the testing environment affected the results. Also one diorite sample was tested in air but first after it had been cycled in water.

1.4 Äspö HRL

Äspö HRL is located near the nuclear power station in Oskarshamn, in the municipality of Simpevarp, Småland. The laboratory started out by testing methods for site investigations and detailed characterizations that will be used to select a suitable site for a future deep repository. Tests are also performed on the equipment that will be used in a repository, like copper canisters and emplacement and retrieval machines. Surrounding the copper canisters there will be a buffer of bentonite clay, which prevents groundwater flow around the canisters as well as protecting them against minor rock movements. The rock types present at the site are igneous rocks and are of four main types, Äspö diorite Småland granite, greenstone and fine-grained granite. At present a test of the deposition procedure is taking place. The canisters with electric heaters are deposited and the holes filled with bentonite. The tunnel is also backfilled and the behavior of the canister, clay and backfill is monitored. Then, after about five years, the first deposition hole is uncovered and scientists can see how the clay, backfill and rock has been affected.

2 Thermal and temperature dependent properties of rock

2.1 Introduction

The thermal properties of rock are important in many geophysical, geothermal and mining applications. Recent studies of the possibility of replacing traditional energy sources like oil with more environmentally friendly energy sources, have found the need for storing surplus energy during summertime for use during the cold period of the year. This seasonal storage often uses water as a medium and storage in rock is an interesting alternative both from the cost and effect point of view. Storage of water at elevated temperatures for an extended period of time means that the temperature of the surrounding rock mass is also increased. Elevated rock temperatures also result from disposal of nuclear waste and thermal methods of enhanced oil recovery.
LPG (Liquefied Petroleum Gas) has been successfully stored in underground caverns since the 60s and even before that it was possible to store ethylene and propylene in unlined caverns. Storage in unlined caverns has worked very well as long as the temperature has been between -15° C and -40° C at a pressure slightly higher than atmospheric. Attempts to store ethylene at a temperature of -100° C and atmospheric pressure led to heavy boil-off of the product (Dahlström, 1992). Storage of LNG (Liquefied Natural Gas) in unlined caverns has not been successful because the normal boiling point of LNG is -162° C, the critical temperature is -82° C and the critical pressure is 4.64 MPa. These temperatures are far below the lowest successful storage temperature in unlined caverns (-40° C). In the two full scale trials that have been reported the boil-off due to migration of LNG into the rock was so large that it was concluded impossible to store LNG in unlined caverns. The cause for the migration has been studied by for example Dahlström (1992) and van den Bogert and Kenter (1994). Storage of LNG in clay has been successful perhaps mostly due to the increase in volume of clay when the temperature decreases (Ogawa et al., 1994). Underground storage of gas has two benefits: decreased environmental effects and increased security. These two facts have made several countries consider underground storage of gas the most beneficial when constructing new facilities (van den Bogert and Kenter, 1994). In Korea there have been recent trials of underground cold storage of food (Park et al., 1999).
All these applications require knowledge of how a change in temperature affects the stability of the cavern itself and the surrounding rock and how the properties of the rock mass change with temperature. A decrease in temperature in a near surface cavern can for example cause subsidence of the ground surface or cause formation of cracks and open joints due to stress release around the cavern which may lead to boil-off of the gas. Both of these effects are economically costly. An increase in the temperature of the rock mass can in turn cause expansion of the rock closest to the cavern, which may lead to failure due to the compressive strength of the rock being exceeded. All this makes it important not to focus only on the thermal properties of the rock, but to consider the effects a change in temperature may have on the physical and mechanical properties as well. Thermal properties, such as conductivity, diffusivity and heat capacity, are properties that are directly dependent on temperature. Several of the mechanical and physical properties are more or less affected by changes in temperature and can be

termed temperature dependent. Thermal expansion is a mechanical property that could be placed in both categories, but in the literature it is usually mentioned with the thermal properties. Both temperature and pressure affect both categories of properties. These two factors often interact so it is not possible to write about the effects of temperature without mentioning the effects of pressure. In Table 1 the properties that are most commonly found from tests in the literature have been listed. Several other properties exist but not all of them are relevant for igneous rocks. Electric properties and formation resisitivity factor are temperature dependent properties of sandstone that were tested by Somerton (1992) but since no reference to testing of these properties for igneous rocks have been found, they have been left out. Latent heat of fusion is another property that has been tested but there is so limited material to be found about the actual tests and results that it also has been left out.

Table 1 Thermal and temperature dependent properties

Thermal Properties	**Temperature dependent properties**	
	Mechanical	**Physical**
Conductivity	Young's modulus	Absolute/relative permeability
Heat capacity	Poisson's number	Porosity
Diffusivity	Tensile strength	Bulk- and pore compressibility
Thermal expansion	Compressive strength	Elastic wave velocity

2.2 Definitions of terms used in the text

Matrix: the dense fine-grained mass surrounding the bigger mineral grains (Loberg, 1992)

α-β-inversion of quartz: Quartz exists in two forms: (1) alpha-, or low, quartz, which is stable up to 573º C and (2) beta-, or high, quartz, stable between 573º C and 867º C. At temperatures between 867º C and 1470º C, beta-quartz changes into tridymite, but the transformation is very slow because bond breaking takes place to form a more open structure. At even higher temperatures the tridymite changes into cristobalite that is stable between 1470º C and 1710º C. The low and high forms of quartz are closely related, with only small movements of their constituent atoms during the alpha-beta transition. The structure of beta-quartz is hexagonal and the structure of alpha-quartz is trigonal. At the transition temperature the framework of beta-quartz twists, resulting in the symmetry of alpha-quartz by atoms moving from special space group positions to more general positions. The high-low transformations require only slight displacements of the tetrahedral groups and occur rapidly. Compositionally, quartz is usually quite pure, with only traces of other elements. In contrast, tridymite and cristobalite may contain up to about one percent by weight of impurities because of the open nature of their framework that easily accommodates other atoms, especially those of aluminium, sodium, potassium, and lithium. (Kingery et al., 1976 and http://www.britannica.com for full address, see reference list)

2.3 Thermal properties

Conductivity

Thermal conductivity (λ) is a measure of the capacity of a material to conduct or transmit heat and is given in W/m·K. The thermal conductivity of crystalline rocks decreases with increasing temperature. The surrounding pressure does not seem to have any influence at lower temperatures. Heuze (1983) reports that a granite that was tested up to 90 MPa at constant temperature showed a 10 percent increase in thermal conductivity. Another granite that was heated from 20º C to 200º C at a pressure of 3 MPa did not show any changes in conductivity, but when the pressure was increased to 50 MPa the conductivity decreased by 22 percent over the same temperature interval. The thermal conductivity varies greatly between different minerals, where quartz has the highest, 7.7 W/m·K, and most others lie between 2.0 and 2.5 W/m·K. The conductivity depends on porosity and mineral content, so that a rock with high porosity has a lower conductivity compared to a rock with the same mineral content but lower porosity (Dahlström, 1992). An average value of the conductivity for granite and gneiss is 3.5 W/m·K. According to Dahlström tests on granites have shown that the conductivity at -100º C is 10 - 20 percent higher than the conductivity at 20º C. The water content does not seem to influence the conductivity of granites, mostly due to the low porosity. For rocks with a high porosity the water content can have a substantial influence on the conductivity, for example an saturated unconsolidated sand can have a conductivity three times the conductivity of the same sand in a dry state.

Heat capacity / Specific heat

The heat capacity (C) is a measure of the capacity of a material to store heat and is given in J/kg·K. Specific heat is the amount of heat required to increase the temperature of water by one degree at standard conditions (15º C and atmospheric pressure). The SI-unit of specific heat is also J/kg·K. The total specific heat of a composite material like rock is the sum of the specific heats of the individual components (Sundberg, 1988). The same is true for the thermal conductivity. In the rock the minerals have the lowest specific heat, 740 J/kg·K, compared with water that has 4180 J/kg·K at 20º C and ice that has 2040 J/kg·K at 0º C (Dahlström, 1992). Porosity and water content are the most important factors of influence. Granite which has a low porosity and thus a low water content has a specific heat of between 730 J/kg·K and 800 J/kg·K at room temperature (Dahlström, 1992). The heat capacity increases with increasing temperature but it is relatively insensitive to changes in surrounding pressure since it is based on mass. Heuze (1983) shows that the heat capacity for granites increases linearly up to the α-β-inversion of quartz (573º C). At higher temperatures the heat capacity seems to be more or less constant. For sinking temperatures the decrease continues to be linear.

Thermal diffusivity

The thermal diffusivity (κ) is a measure of the capacity of a material to level out differences in temperature and it is given in m^2/s. The relationship between the diffusivity and the preceding properties is as follows:

$$\kappa = \frac{\lambda}{C}$$

As can be seen from this relationship the thermal diffusivity is proportional to the thermal conductivity and is inversely proportional to the heat capacity. Thermal diffusivity is strongly dependent on temperature, the diffusivity decreases value as the temperature increases. Heuze (1983) has collected and compiled data from several authors on tests on granite and has found that the diffusivity is lowest at 573º C, which coincides with the α-β-inversion of quartz. Inada and Sterling (1989) found the diffusivity of granite and andesite to be constant over the temperature interval 30º C to 80º C. Dahlström (1992) has examined the behaviour of the diffusivity at temperatures below 0º C and has found that it, similar to the thermal conductivity, increases with decreasing temperature.

Thermal expansion

The coefficient of thermal expansion (α_t, β) is defined as the increase in length (area, volume) over a given increase in temperature divided by the original length (area, volume) (Jumikis, 1983). The linear coefficient is defined as follows:

$$\alpha_t = \frac{\Delta L}{L \cdot \Delta T} \quad (1/^{o} C) \qquad (1)$$

For homogenous bodies the coefficient of volume expansion is defined as

$$\beta = 3\alpha_t, \qquad (2)$$

or more completely as

$$\beta = \frac{\Delta V}{V_0 \cdot \Delta T} \quad (1/^{o} \text{C}). \qquad (3)$$

Most igneous rocks with an isotropic extension in all directions can be assumed to be homogenous. Thermal expansion of igneous rocks is a function of crack porosity, heating rate, previous maximum temperature, mineralogical composition and preferred crystal orientation (Richter and Simmons, 1974). Richter and Simmons studied the effects of heating/cooling rates, repeated heating/cooling cycles, microcracks, grain size and mineralogical composition on the thermal expansion of igneous rocks over the temperature interval 25º C - 550º C at atmospheric pressure. They heated their samples at a rate of 1 - 2º C/min for 30 minutes and then kept the temperature constant for 60 minutes. Each data point was the average of the sample temperature and length during the last 40 minutes of the 60 minute interval in which the temperature remained constant. From their tests they concluded that for heating rates ≤ 2º C/min and temperatures below 250º C the expansion curve can be repeated but it might show some hysteresis. This means that the curve for heating of the sample looks the same every time but the cooling curve shifts slightly every time. At higher temperatures or higher heating rates new cracks and thus permanent strains are introduced in the sample. This is shown in Figure 1, where the cooling curve of cycle 2 - 5 is an average of these 4 cycles.

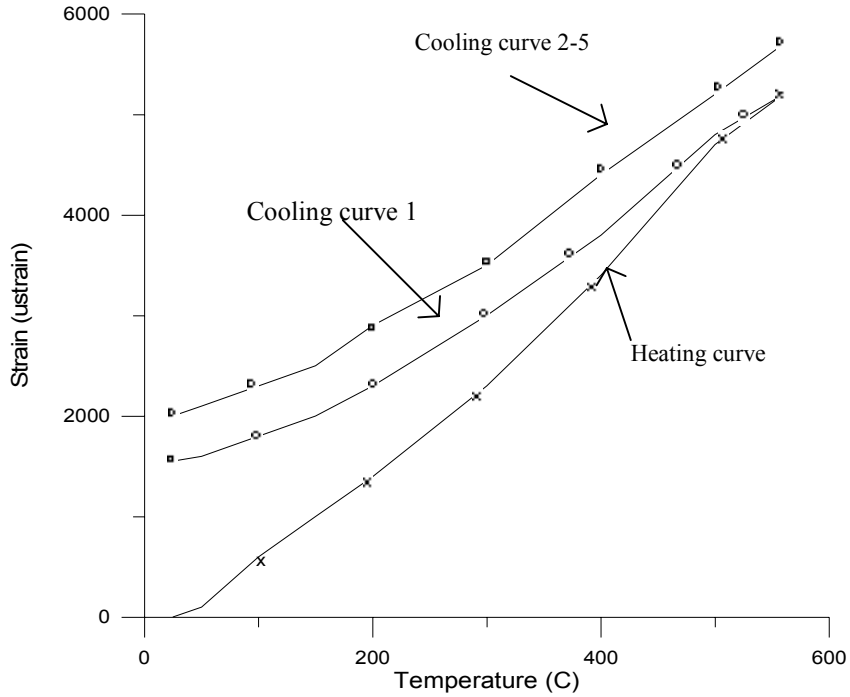

Figure 1 *Temperature influenced strain cycles (after Richter and Simmons, 1974)*

Another result of their tests was that the measured coefficient of thermal expansion almost coincided with the coefficient determined theoretically from the constituent minerals. Recycling to the same temperature produces additional cracks until a steady state is reached after 2 -5 cycles. They also found that the coefficient decreased with an increasing number of cycles, and that the residual strain did not influence the value of the coefficient. When the sample has been heated enough for permanent strains of about 300με to form the coefficient starts to decrease. The authors also concluded that the thermal expansion of igneous rocks should be viewed in relation to the thermal history of the sample, i.e. the previous maximum temperature to which the sample has been subjected. They also found that the coefficient depended inversely on the microcrack porosity, which in turn varies exponentially with the maximum cycle temperature. Mineral composition and initial crack porosity probably influence the formation of new cracks in the sample (Simmons and Cooper, 1978). They found that rocks with low initial crack porosity have the largest increase in crack porosity during cyclic heating up to 900º C at atmospheric pressure.
Crystalline rocks like granite are extremely sensitive to formation of microcracks due to heating because of the differences in thermal properties of the constituent minerals. Microcracks do not always form unless the temperature exceeds a threshold value, which lies between 75º C and 100º C for granite. The threshold value depends on the constituent minerals and the state of the microcracks before heating (Aversa and Evangelista, 1993, and Johnson et al., 1978). At temperatures higher than the threshold value microcracks always form. According to Cooper and Simmons (1977), there are two types of cracks forming when the temperature changes: cracks that are caused by the thermal gradient in the sample and cracks caused by cyclic heating. The first type is due to inhomogeneous strains caused by inhomogeneous temperature in the sample. The second type is due to inhomogeneous strains caused by differences in thermal expansion at the grain boundaries and this type cannot be avoided by low heating rates.

Thermal expansion measured at atmospheric pressure has been reported irreversible after heating above room temperature and the coefficient of thermal expansion is usually much larger than the coefficient calculated from the constituent minerals. Walsh (1973), who determined theoretical upper and lower bounds for thermal expansion of polycrystalline materials, observed that determinations of the coefficient of thermal expansion at atmospheric pressure generally are above the theoretical upper bound. Walsh suggested that the irreversible effects and the high values could be caused by microcracking in the sample caused by internal stresses. Therefore Wong and Brace tested samples that were subjected to high surrounding pressures, up to 600 MPa, over the temperature interval 2º C - 38º C. In this interval the thermal expansion should be linear. If the curve is non-linear or residual strains remain after the completion of the heating cycle this means that thermal cracking has occurred. Wong and Brace also tried to determine the surrounding pressure needed to prevent microcracking. They succeeded in making the strains reversible and their values of the coefficient lay very close to the theoretically determined value. They concluded that the surrounding pressure had small influence as long as it was above a critical pressure, which is the lowest pressure needed to prevent thermal cracking and other irreversible effects. The critical pressure depended on both rock type and the thermal history of the sample. The critical pressure for granite lies between 50 and 150 MPa. Thermal cracking depends not only on the size of the load but also on its direction. Ehara et al. (1983) found that the load affected the thermal cracking parallel to the load direction less than the cracking perpendicular to the load direction. They also found that the sample "remembered" previous cycles as long as the load was kept constant, but that it did not remember the stress situation of the previous cycle after the external loading had been changed. Inada and Sterling (1989) determined several properties, among them the coefficient of thermal expansion, of granite and andesite in the laboratory. The coefficient was determined by cyclically heating and cooling dry and saturated samples between 15º C and 100º C. Residual strains at room temperature were measured after the first cycle. These strains converged to a constant value as the cycle was repeated. A comparison between the granite and the andesite shows that the granite is more prone to thermal cracking than the andesite, and that wet (saturated) samples are more sensitive than dry samples. The residual strain for granite was 100 με for dry samples and 240 με for wet samples. They also concluded that the average thermal expansion for every degree of increase in temperature seems to increase at higher temperatures.

The observation by Walsh (1973) that there is a difference between calculated and measured values of the coefficient of thermal expansion and the results obtained by Richter and Simmons (1974), which states a good agreement between calculated and measured values seem to be at odds with one another. The discrepancy may be explained by the fact that Richter and Simmons were among the first to recognize the importance of slow heating rates for avoiding microcracking of the samples. The results which Walsh have used have come from researchers who have not realized this and thus have used a too high heating rate causing microcracking and a larger expansion than theoretically calculated.

Based on the mineral composition a theoretical determination of the coefficient of thermal expansion can be done. Several methods have been presented during the years. Turner's method is straightforward and quite simplified (Kingery et al., 1976), while Walsh's method is more advanced and takes the internal stresses caused by the thermal gradient across the sample into consideration, which Turner's equation does not. Turner's equation originates from ceramics but is also applicable to other polycrystalline materials such as rock. A few assumptions concerning the material have been made:

1. Isotropic phase distribution
2. The expansion of the phases is independent of grain size and shape
3. No internal disruptions occur
4. The bulk moduli of the components are approximately equal

The coefficient of thermal expansion of the aggregate according to Turner (Kingery et al., 1976) is

$$\alpha_r = \frac{\sum \alpha_i K_i F_i / \rho_i}{\sum K_i F_i / \rho_i} \tag{4}$$

where

α_i is the coefficient of thermal expansion for the constituent materials

K_i is the bulk modulus for the constituent materials

F_i is the weight fraction for the constituent materials

ρ_i is the density for the constituent materials

When comparing values of α_r calculated using Turner's equation with values calculated from more complex formulae for the thermal expansion of an aggregate they were found to agree within a few percent (Richter and Simmons, 1974).

Walsh's method is constructed so that the only parameters needed to calculate the upper (α_U) and lower (α_L) bounds of the thermal expansion are the mineral composition and the anisotropic elastic and thermal expansion properties of the constituent minerals. This means that the single-crystal stiffness and compliance tensors, the thermal expansion tensors and the partial volumes of the mineral components need to be calculated.

The upper and lower bound of the thermal expansion according to Walsh (1973) is

$$\alpha_U = \alpha_m + \Delta\alpha \tag{5}$$

$$\alpha_L = \alpha_m - \Delta\alpha \tag{6}$$

where

$$3\alpha_m = \langle\alpha\rangle + \frac{\beta_U - \beta}{\beta_U - \beta_L}\left(\frac{3\langle c\alpha\rangle}{\langle c\rangle} - \langle\alpha\rangle\right) \tag{7}$$

$$3\Delta\alpha = \frac{(\beta - \beta_L)^{1/2}(\beta_U - \beta)^{1/2}}{\beta_U - \beta_L}\left[(\beta_U - \beta_L)\left(\langle c\alpha^2\rangle - \frac{\langle c\alpha^2\rangle}{\langle c\rangle}\right) - \left(\frac{3\langle c\alpha\rangle}{\langle c\rangle} - \langle\alpha\rangle\right)^2\right]^{1/2} \tag{8}$$

and α_m is the average value. Angle brackets denote a volume-weighted average over all constituents, c and α are the stiffness and thermal expansion tensors, and β is the bulk compressibility.
Quartz is the mineral that influences the coefficient of thermal expansion the most because it has a much larger thermal expansion (0.36 %) than most other minerals (~0.1 %) (Clark, 1966). Somerton (1992) tested sandstones with a quartz content of 50 and 80 per cent, and found that the thermal expansion coefficient for the sandstones was approximately equal to that of quartz. If the rock contains no quartz it is the mineral with the highest concentration that decides the coefficient. The coefficient of thermal expansion varies depending on the temperature interval for which it has been determined. This can be explained by the fact that it does not vary linearly with temperature. Dahlström (1992) made measurements at temperatures below 0° C. He then determined the coefficient of contraction and concluded that it decreased with decreasing temperature. Several researchers have determined the axial coefficient of thermal expansion for sandstone and granite with different temperature intervals and different results. An example of the differences can be found in Table 2. No reference to testing of the volumetric coefficient of thermal expansion has been found in the literature.

Table 2 Coefficients of thermal expansion of two rock types, determined by different researchers.

Author	Rock type	Temperature interval (°C)	Coefficient of linear thermal expansion, α
Somerton (1992)	Dry sandstone	100 - 200	$15 \cdot 10^{-6}$
Jumikis (1983)	Dry sandstone	25 - 100	$36 \cdot 10^{-7}$ - $65 \cdot 10^{-7}$
Richter, Simmons (1974)*	Granite	25 - 200	$77 \cdot 10^{-7}$ - $112 \cdot 10^{-7}$
Jumikis (1983)	Granite	25 - 100	$34 \cdot 10^{-7}$ - $66 \cdot 10^{-7}$

* Richter and Simmons (1974) measured the axial coefficient but reported the volumetric coefficient as three times the axial coefficient. Their volumetric values are $23.2 \cdot 10^{-6}$ - $33.6 \cdot 10^{-6}$ 1/°C.
The thermal expansion of rocks can be used to study other parameters. Mahmutoglu (1998) studied the effects of cracks on the strength. He tested samples of marble and sandstone that had been cyclically heated up to 600°C between 0 and 16 times. The purpose of the cyclical heating was to decrease the binding between the grains in order to simulate cracks in the rock and thus be able to discuss the changes in mechanical behavior that exist in a jointed rock mass. He tested for example the compressive and tensile strength and found that the strength decreases gradually with an increasing number of heating cycles.

2.4 Temperature dependent properties

2.4.1 Mechanical properties

Young's modulus

The effect of temperature on Young's modulus depends on rock type. According to Lama (1978) a decrease in temperature increases Young's modulus while an increase in temperature not only results in a decrease in Young's modulus but also in a changing of the curve, see Figure 2.

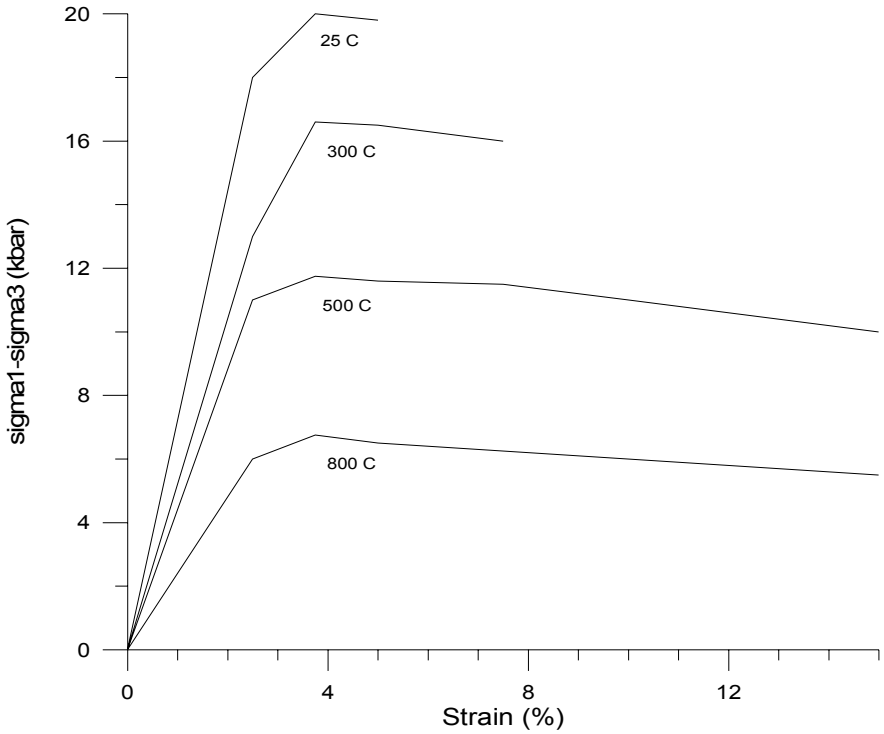

Figure 2 *Behavior of Young's modulus at different temperatures*

Barbish and Gardner (1969) have come to the same conclusion with the addition that Young's modulus for igneous rocks at room temperature (they tested gabbro) depends on the previous maximum temperature to which the sample has been subjected. The reason for this is that microcracks form in the matrix of the rock due to differential expansion of the constituent minerals. Heuze (1983) also found that Young's modulus decreases with increasing temperature, but that increasing the surrounding pressure positively affects the decrease. Mahmutoglu (1998) found that the elastic modulus decreased with an increasing number of heating cycles. After 16 cycles up to 600° C the elastic modulus for sandstone had decreased by 54 %. If the temperature is decreased below 0° C instead, Young's modulus increases rapidly at first but flattens out between -120° C and -150° C (Dahlström, 1992). This can be explained by water freezing to ice from the surface of the sample inwards and when the temperature decreases the pores contract and lower the freezing point. The Young's modulus of the ice also contributes to the increase in total Young's modulus. These effects make it important to test the samples with the in-situ water content. At temperatures above 0° C the water content does not seem to have any influence for rocks with a high porosity (Somerton, 1992), so it should not present a problem for granite, which has a low porosity.

Poisson's ratio

According to Lama (1978) Poisson's ratio varies with temperature in about the same way as Young's modulus, i. e. an increase in temperature decreases Poisson's ratio. For granites no clear relationship with temperature or pressure has been established (Heuze, 1983). Poisson's ratio does not seem to be as affected by a decrease in temperature below 0° C as Young's modulus. Poisson's ratio does increase when the temperature is decreased from 0°C to -10°C, but at further decrease of the temperature Poisson's ratio remains constant (Dahlström, 1992).

Compressive strength

The compressive strength decreases with increasing temperature to reach a zero value at the melting point. For granites the water content does not seem to influence the compressive strength. Heuze (1983) came to this conclusion after having tested granites at an effective pressure of 300 MPa up to 265° C. Tests on gabbro at temperatures up to 1000° C showed that wet samples even had slightly higher strength than dry samples. Heuze adds that the water content might be important in long term loading. If the temperature is decreased below 0° C instead, the compressive strength continues to increase down to -120° C and then remains relatively constant or decreases slightly if the temperature is decreased further (Dahlström, 1992). The amount of increase depends on rock type, porosity and water content. For granites with a low porosity the strength increase is smaller compared with sandstones, which have a higher porosity. When comparing samples of the same rock type but with different water content the saturated samples had a higher strength increase than the partially saturated samples.

Tensile strength

The tensile strength for granites is also adversely affected by an increase in temperature (Heuze, 1983). From a tensile strength of ~14 MPa at room temperature it decreased to 2 MPa at 800° C. Dahlström (1992) states that the tensile strength at temperatures below 0° C has the same relative increase as the compressive strength over the same temperature interval. From this he concludes that the relationship that exists between the tensile and the compressive strength at room temperature is valid also at temperatures below 0° C. As for the compressive strength wet samples have a larger increase in strength than dry samples do.

2.4.2 Physical properties

Permeability

The ability of a porous material to transmit fluids through it is known as permeability, where the unit is given in m^2. Absolute permeability is the fluid-flow capacity of a medium to a single fluid with which the porous medium is fully saturated. The absolute permeability decreases with an increase in both pressure and temperature (Somerton, 1992). Homand-Etienne and Troalen (1984) tested granites and found that the inner permeability increased with increasing temperature. They noted three different stages with different rates of increase. The first slow increase (up to 150° C) they explained as failure in some of the grains. The second, slightly more rapid increase (between 150°C and 200°C) was explained as microcracks between the grains propagating and joining each other and the third stage (between 500°C and 600°C) of rapid increase was explained as microcracks forming inside the mineral crystals. The first increase occurs at lower temperatures the larger the grain size of the rock.

Porosity

Porosity is the part of the total volume of a material that is available for storing fluids. Total porosity is the pore volume divided by the total volume. Some parts of the pore volume might be isolated and not connected to the rest. Because of this it is more common to speak of effective porosity, which is defined as available pore volume divided by total volume. The porosity of a rock depends on mineral content and mode of formation. In crystalline rock pores are formed between the grains as the magma cools but can also form due to internal stresses. Porosity decreases with increasing effective stresses and also due to increasing temperature. These factors cooperate so that the amount of reduction in porosity caused by stress increases with increasing temperature. The effect of just increasing the temperature might be an increase in porosity due to cracking between the grains due to their differential thermal expansion (Somerton, 1992). This has also been studied by Johnson et al. (1978) and they concluded that, for granites, the increase in porosity at temperatures below the α-β-inversion of quartz is caused by microcrack formation while the increase at higher temperatures is explained by propagation of already formed cracks since the formation of microcracks decreases at higher temperatures.

Bulk- and pore compressibility

The compressibility of a rock depends on the compressibility of the grains, pores and cracks. Cracks in the rock have a great influence but sometimes the grain size can be the determinant factor. Lama (1978) refers to a test by Brace in which he tested the compressibility of two granites with different porosity and grain size. Generally the compressibility is larger for more porous rocks, but in this case the opposite was true. The granite with the lower porosity and the larger grains had twice the compressibility of the other granite, which had a porosity four times higher and grains about a third of the size. From this Brace concluded that a part of the compressibility was due to grain boundaries. The surrounding pressure also influences the compressibility. The compressibility at low pressures can be several times the compressibility at higher pressures. This can be explained by the elimination of the influence from the cracks when the pressure increases to about 2-3 kbar (200-300 MPa), but that the influence of the pores is not affected by this pressure (Lama, 1978). For granites there is not much written of how temperature changes affect the compressibility, but for sandstones the compressibility seems to increase with increasing temperature. The amount of increase depends on both mineral composition and porosity so that a low quartz content and a decreasing porosity result in a lower increase of the compressibility (Somerton, 1992).

Elastic wave propagation

The effects of temperature have been tested on two types of elastic waves, dilatational or longitudinal wave (P-wave) and shear wave (S wave). An increase in temperature decreases the velocity of propagation for both waves. The longitudinal wave propagation velocity is affected by several factors: the elastic properties of the different crystals, discontinuities in the sample, erosion or microcracks (Homand-Etienne and Troalen, 1984). They also found that the velocity of the P-wave decreased linearly up to 400° C with a sharper decline between 500° C and 600° C. In granites, it is the differential expansion of quartz and feldspar that is most important for the formation of microcracks and their propagation at temperatures below the α-β-inversion of quartz. The velocity of the P-wave decreases more rapidly the larger the grain size of the sample. The smaller the grain size the smaller the absolute difference in expansion, which means that smaller tensile stresses form and that reduces the risk of the tensile stresses between the crystals becoming larger than the tensile strength. At the freezing point there is a sharp increase in velocity for wet samples. Lama (1978) claims that the only correct measurements of changes in velocity due to temperature are the ones that have been made at a surrounding pressure larger than 1 kbar (100 MPa). He has come to this conclusion because defects in the rock such as cracks or bad contact between the grains are cancelled by the pressure and this means that the waves can propagate freely through the rock mass.

3 Tests

3.1 Test site description

The samples were taken from pilot holes that were cored at the location of the deposition holes in the Prototype Repository tunnel. This tunnel is located at a depth of about 450 m. The rock types in the cored holes are diorite and granite, and samples from both rock types were tested.

3.2 Sample preparation

The samples were chosen as evenly along the boreholes as possible. This was done to get representative values of the coefficient of thermal expansion along the hole. The samples tested are listed in Table 3, along with the depth of sampling from invert level of tunnel. Four samples were chosen as replacements in case anything went wrong. These were not prepared with gauges, and are noted as sawn only in the Table 3. The comments in the table refer to how the samples were tested. If there is no comment they were cycled twice, without and with load and in water. The diameter of the sample is 45 mm and the height is 90 mm.

Table 3 Samples chosen for testing

Sample no	Drillhole no	Depth (m)	Comments
D1	KA3551G	1	
D3	KA3551G	3	Load only
D4	KA3551G	5	Sawn only
D5	KA3563G	1	Load only + air
D7	KA3563G	3	
D8	KA3563G	7	Sawn only
D9	KA3575G	2	
D11	KA3575G	5	
G1	KC0045F	3	
G2	KC0045F	5	Sawn only
G5	KC0045F	9	
G9	KC0045F	16	Air
G12	KC0045F	25	Sawn only

The strain was measured with strain gauges, which were glued to the samples as shown in Figure 3.

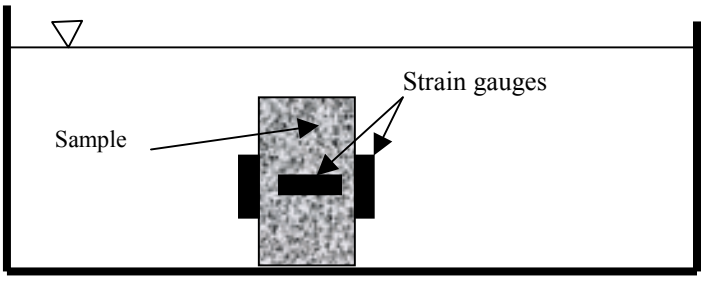

Figure 3 *Position of strain gauges on sample*

Since the diorite is quite coarse grained gauges that were 12.5 mm long were used. The strain gauges used were electric resistance gauges with a resistance of 120 Ω. (Type: CEA-06-500UW-120) The gauges were attached to the samples by using an adhesive (glue). To secure proper curing of the glue the sample with the gauge had to be heated above room temperature, and also be put under pressure. High temperatures give a shorter curing time, but the samples were not supposed to be subjected to any heating before the actual tests. The pressure was achieved by using a clamp. It was decided to cure the glue at a temperature of 37° C for 3 hours, which should give sufficient curing according to the manufacturer. To assure a creep-free performance the samples would have had to be post-cured for 2 hours at a temperature of 15°C above the maximum operating temperature but for the same reasons as above this was not done. To further improve water resistance, the gauges were covered by a thick layer of silicon. The accuracy of the whole measuring system was about 1%.
The cables used were made of PTFE (polyterafluoroethylene) or Teflon. This type was selected because they can operate at higher temperatures than standard PVC cables and also operate when submerged in water. During testing care was taken that the cables would not come in contact with the water, but as a safety measure it was decided to use Teflon cables.
The connection used was a full bridge, which gives a more sensitive measuring system. The full bridge connection also allows improved temperature compensation and better cancellation of unwanted signals (Window and Holister, 1982).

3.3 Equipment

The equipment used for the tests was a loading device, a container filled with water, strain gauges and measuring equipment and an immersion heater.
Loading of the samples was achieved by a load setup (Figure 4) with a spring transmitting the load to the samples. The largest stress at the depth (~500 m) from which the samples have been collected is 10 - 15 MPa. These stresses were not possible to achieve with our loading device, so a stress of 3.8 MPa was used, which corresponds to a load of about 6 kN. This load is the highest load we were able to achieve with the load set up used.

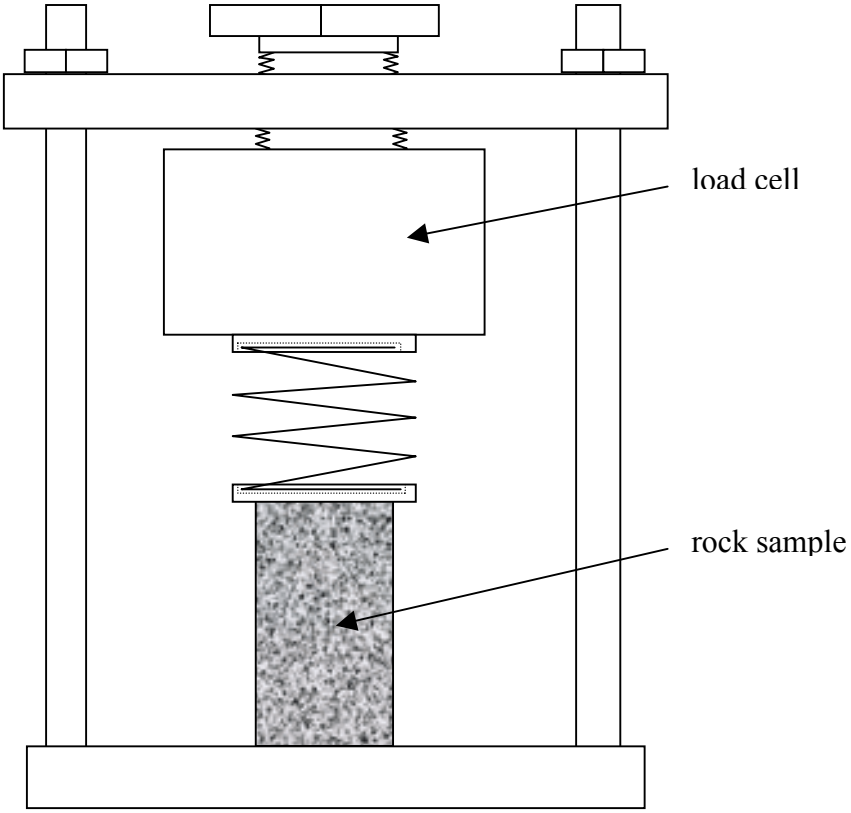

Figure 4 *Loading device*

3.4 Execution of tests

The tests were performed so, that in the first cycle the samples were heated up to 50° C and 70° C without loading and in the second cycle they were loaded with 6 kN (3.8 MPa) and heated up to 50° C and 70° C again. After the water had reached each desired temperature it was left in the oven between 8 and 12 hours so the heat could spread evenly through the sample. Strain measurements were made continually during heating and cooling. The maximum working temperature of the load cell is 70° C, so this temperature was chosen as the maximum. The strain in the sample at room temperature before heating was calibrated to zero. Two samples were tested with the load without earlier cycling, one of these was also cycled in air after the initial cycling in water. The testing of the granite followed the same pattern except that there was no samples cycled with the load only. One of the granite samples was cycled in air instead of water to determine if there is a difference in behavior. The testing is schematically shown in Table 4. As an example take one of the four diorite samples. The vertical arrow (furthest to the left) means that the sample was first cycled without load from 20°C to 70°C and then back down to 20°C again. The horizontal arrow means that it was then loaded to 3.8 MPa followed by another cycle to 70°C, shown as the other vertical arrow. In the first test the oven was used to heat the water but it was discovered that the heating was so slow that the water evaporated. It was decided to heat the water to the desired temperatures using an immersion heater instead and using the oven for maintaining the temperature over the time span necessary for leveling out the temperature differences in the sample.

Table 4 Execution of tests

Temperature	Diorite		Granite	
	Axial load		Axial load	
	0 MPa	3.8 MPa	0 MPa	3.8 MPa
20° C	4 samples		3 samples	
50° C				
70° C				
20° C		2 samples		
50° C				
70° C				
Total number of samples:	4+3+2 = 9			
Total number of strain gauges:	$9 \times 4 = 36$			

3.5 Strain measurements

Measurement of the strain was made every 10 s, and was saved to file every hour throughout the heating and cooling cycles. Since it was not possible to include the temperature in these measurements it was checked at intervals and the present temperature, sampling time and real time was noted. The measurement protocols can be found in Appendix 1.

3.6 Evaluation methodology

Each measurement file consisted of 360 values of the load, the axial strain and the tangential strain respectively. For each measurement file an average value was calculated and the reference strain was subtracted (in the cases where it was not zero). The average values for the load, axial strain and tangential strain at the different temperatures were corrected by subtraction of the temperature correction given by the manufacturer of the gauges (Equation 8). The base files for all samples can be found in Appendix 2. The first four columns of Table 5 below is an example of what a base file looks like.

$$\varepsilon_0 = -32.2 + 2.77 \cdot T - 6.57 \cdot 10^{-2} \cdot T^2 + 3.67 \cdot 10^{-4} \cdot T^3 - 4.73 \cdot 10^{-7} \cdot T^4 \qquad (9)$$

The values were also adapted to the rock mechanics sign convention by adding a minus sign to all values. The corrected values were then used to calculate the volumetric strain and curves were drawn of the axial, tangential and volumetric strain. The volumetric strain is defined as:

$$\varepsilon_{\text{vol}} = \varepsilon_{\text{axial}} + 2 \cdot \varepsilon_{\text{tangential}} \qquad (10)$$

An example of a file for sample G9 can be found in Table 5.

Table 5 Adapted measurement file for sample G9

				temperature correction	
temp	**load**	**ras1**	**korr axs1**	**ras1**	**axs1**
21.7	6.04	16.96	-59.40	17.58	-58.78
21.8	6.04	17.06	-59.59	17.72	-58.93
53.8	5.94	-104.85	-168.56	-125.00	-188.71
51.8	5.94	-104.95	-168.60	-122.35	-186.00
51.8	5.94	-104.71	-168.02	-122.11	-185.42
71.9	5.89	-193.61	-248.52	-242.52	-297.43
72.2	5.89	-195.30	-250.88	-244.72	-300.29
72.4	5.89	-195.64	-251.51	-245.39	-301.26
53.8	5.92	-118.07	-182.19	-138.23	-202.35
55.2	5.92	-113.12	-178.76	-135.27	-200.91
21.8	6.00	12.23	-63.91	12.89	-63.25
21.6	6.00	15.89	-61.52	16.46	-60.95

	Rock mechanics sign convention		
temp	**axs1**	**ras1**	**vol**
21.7	58.78	-17.58	23.62
21.8	58.93	-17.72	23.49
53.8	188.71	125.00	438.72
51.8	186.00	122.35	430.70
51.8	185.42	122.11	429.64
71.9	297.43	242.52	782.47
72.2	300.29	244.72	789.73
72.4	301.26	245.39	792.05
53.8	202.35	138.23	478.80
55.2	200.91	135.27	471.44
21.8	63.25	-12.89	37.47
21.6	60.95	-16.46	28.03

In Table 5, axs1 denotes the axial strain measured on the sample connected to channel 1, and ras1 the tangential strain from the same sample. Korr axs 1 denotes that the starting value (or calibration value) has been subtracted from the raw data. In the vol-column the volumetric strain has been calculated according to Equation 9.

4 Results

4.1 Evaluation of measurement data

Figures 5, 6 and 7 are examples of what the strain curves look like. In these figures the strain developments in the sample for the unloaded and loaded cycle have been plotted together. Temperature is on the X-axis and strain on the Y-axis. In all diagrams positive strains or an increase in strain means compression.

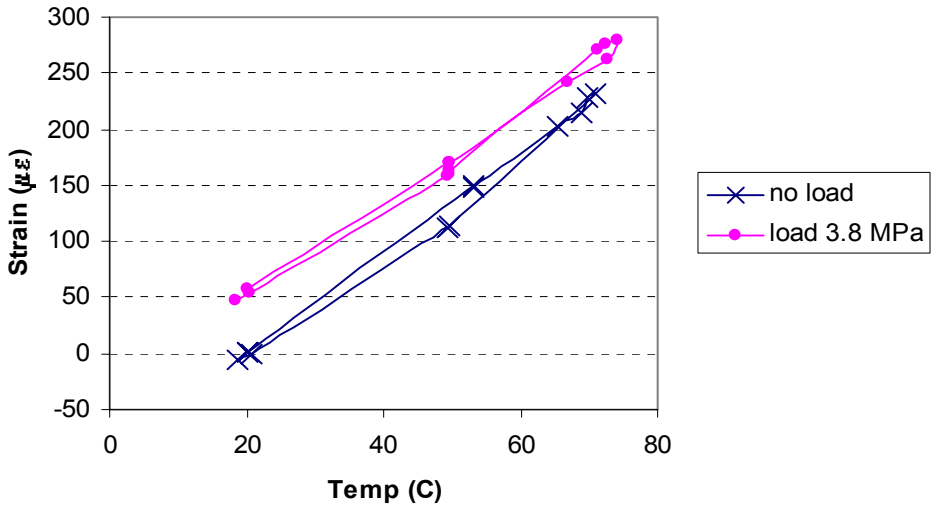

Figure 5 *Axial strain of granite sample G1.*

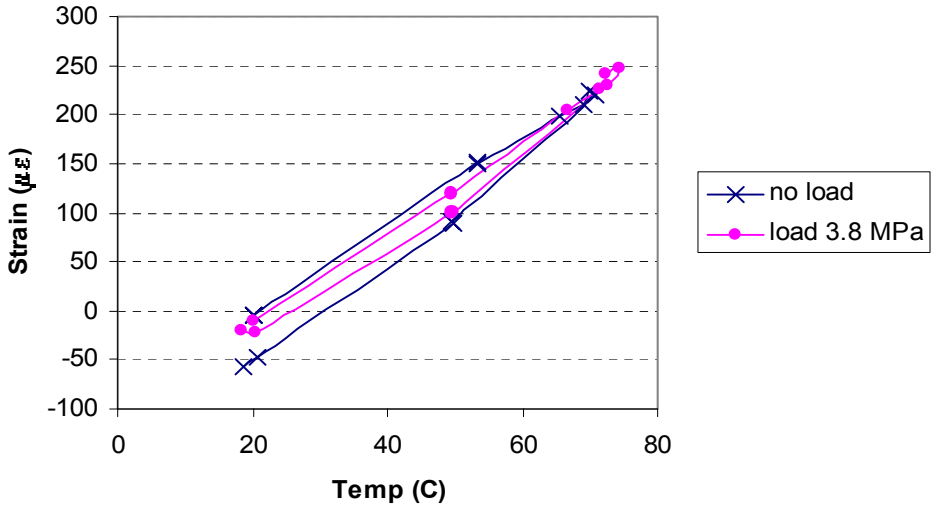

Figure 6 *Tangential strain of granite sample G1.*

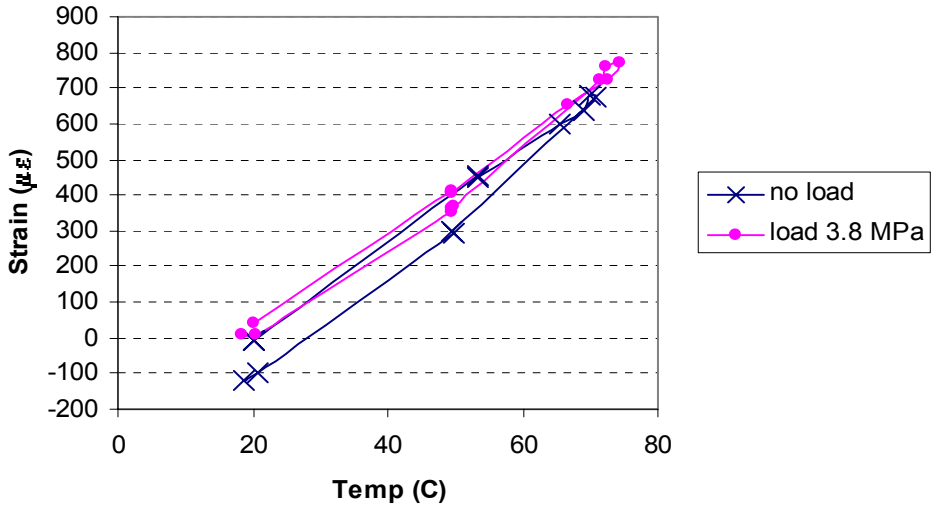

Figure 7 *Volumetric strain of granite sample G1.*

In the above figures the reason some of the curves start at negative values is that the strain gauges were calibrated in room temperature in air and when immersed in water, the sample and the gauges adapted to the temperature of the water, which was somewhat colder than the temperature in the room. This caused extension of the gauges which is seen in the figures as a starting point below zero. The curves representing the loaded cycle is also influenced by this and also by the loading process which for the axial gauges means an increase of the initial strain (compression), and for the tangential gauges a decrease in initial strain (extension).
A line showing the general trend of the curve was inserted into the diagram and the equation of the line was determined. The average axial and volumetric expansion between 20°C and 70°C was then calculated using the equation of that line. The coefficient of thermal expansion was then calculated by Equation 1 and 2. The coefficients were calculated for both unloaded and loaded conditions for both the axial and volumetric case. As a summary the coefficients for all diorite and granite samples were collected in Tables 6 and 7 and also plotted in Figures 8, 9, 10 and 11 to show the differences between the samples and also between the two loading conditions.

Table 6 Summary of axial coefficient of thermal expansion

Diorite	**unloaded**	**loaded**	**Granite**	**unloaded**	**loaded**
D1	3.89E-06	5.91E-06	G1	4.01E-06	4.13E-06
D9	3.85E-06	4.61E-06	G5	5.42E-06	3.67E-06
D11	4.86E-06	4.90E-06	G9	4.72E-06	4.63E-06
D7	4.03E-06	4.94E-06			
D5	-	4.38E-06			
D3	-	5.03E-06			
average	4E-06	5E-06	average	5E-06	4E-06
st dev	5E-07	5E-07	st dev	7E-07	5E-07

Table 7 Summary of volumetric coefficient of thermal expansion

Diorite	unloaded	loaded	Granite	unloaded	loaded
D1	1.13E-05		G1	1.33E-05	1.37E-05
D9	8.28E-06	1.06E-06	G5	1.59E-05	1.04E-05
D11	2.73E-06	4.51E-06	G9	1.48E-05	1.47E-05
D7	1.09E-05	1.44E-06			
D5	-	1.07E-06			
D3	-	1.58E-06			
average	8E-06	11E-06	average	15E-06	13E-06
st dev	4E-06	4E-06	st dev	1E-06	2E-06

In Figures 8 and 9 the axial and volumetric coefficient for the diorite samples can be seen. The strain diagrams for all the samples can be found in Appendix 3.

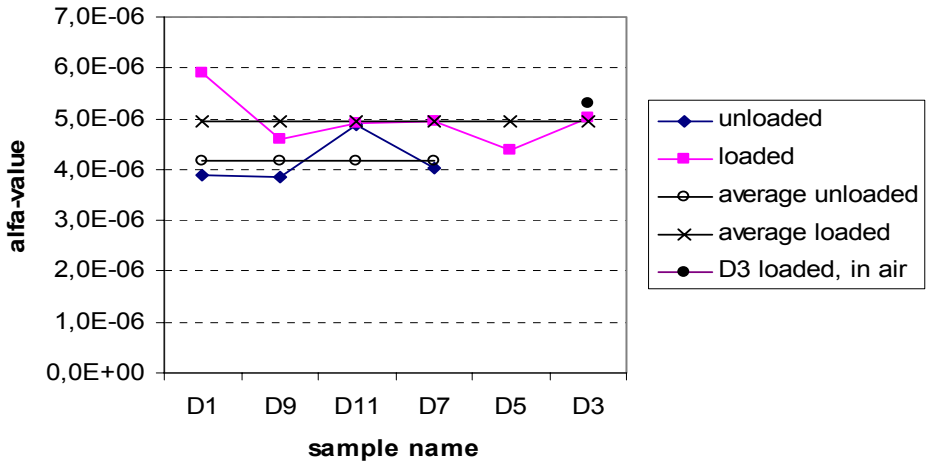

Figure 8 *Differences in the axial coefficient of thermal expansion for diorite*

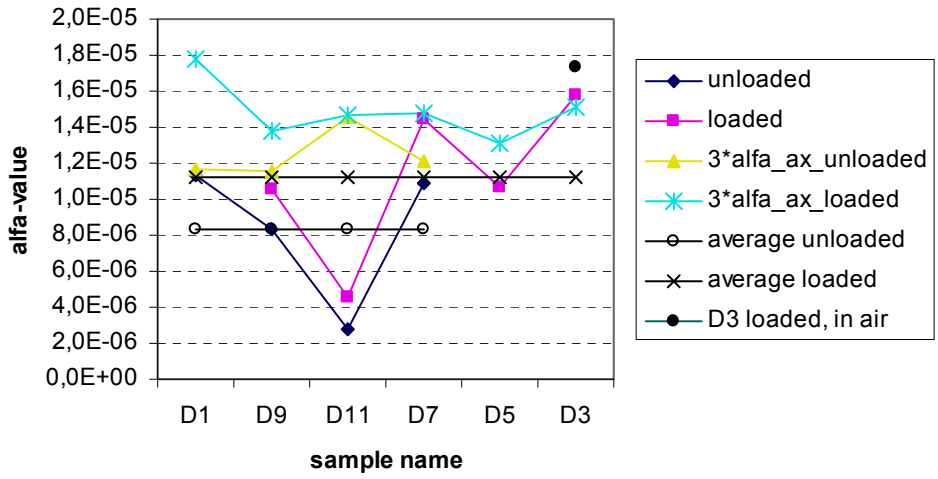

Figure 9 *Differences in the volumetric coefficient of thermal expansion for diorite*

No value of the volumetric coefficient for D1 (loaded) could be obtained due to malfunction of the tangential strain gauge. The axial coefficient for the loaded condition is higher than the coefficient for the unloaded condition for all samples except D11, where they coincide. The volumetric coefficient is higher under loaded conditions for all samples, see Figure 9.
In Figures 10 and 11 the axial and volumetric coefficient for the granite samples can be seen.

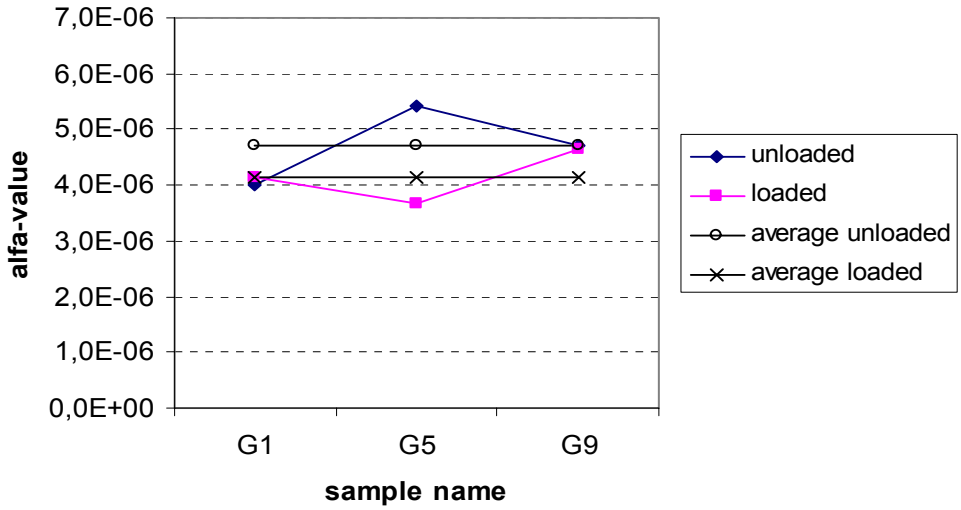

Figure 10 *Differences in the axial coefficient of thermal expansion for granite*

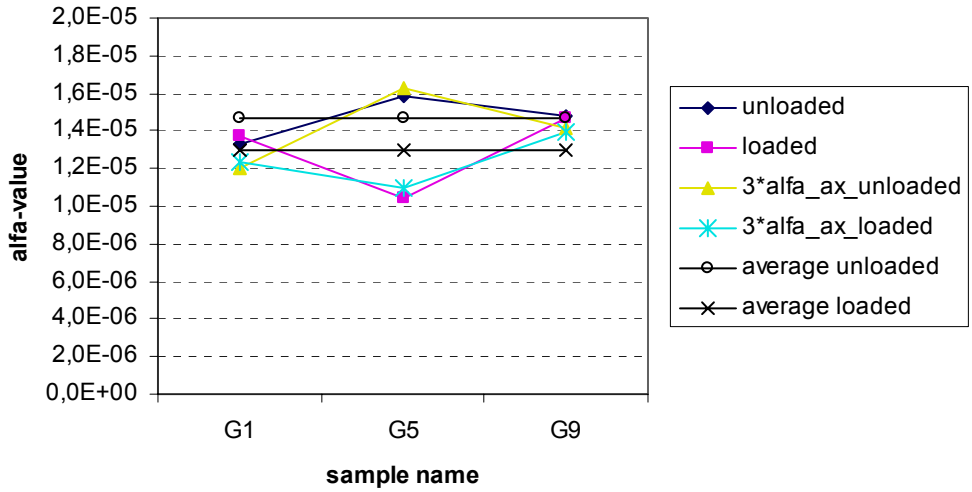

Figure 11 *Differences in the volumetric coefficient of thermal expansion for granite.*

For the granite the axial and volumetric coefficient for the unloaded and loaded conditions are in good agreement for samples G1 and G9, see Figures 10 and 11. The results from the loaded cycle of sample G5 are uncertain due to malfunction of the strain gauges.
As can be seen from Figure 9 the volumetric coefficients for sample D11 and to some extent also sample D9 are lower than the values for the other samples. This can be explained by the fact that the tangential strain gauges on these two samples (which were tested simultaneously) partly malfunctioned during testing. The same can be seen in Figures 10 and 11 where the value for sample G5 (loaded) deviates from the others due to malfunction of both the axial and tangential strain gauges so that only the heating cycle gave values worth interpreting.
The assumption of the volumetric strain as three times the axial strain (Equation 2) agrees better with the measured values for the granite than for the diorite, see Figures 9 and 11. For the unloaded diorite samples Equation 2 agrees better with the measured values than for the loaded samples. The difference between diorite and granite could be explained by the fact that the diorite has a large grain size, which makes the assumption of a homogenous body with isotropic extension less true than for the small-grained granite. Non-isotropic expansion of the large grains could contribute to the difference between the unloaded and loaded condition by introducing microcracks in the sample as it is loaded.
In Table 8, a summary of the coefficients for both rock types and loading conditions are given. The averages in this table are calculated for each rock type to ease comparison between them. As can be seen the axial coefficients do not differ between the rock types, which also means that the volumetric coefficient calculated by using Equation 2 is the same. The deviation of the measured volumetric coefficient (for diorite) from the calculated value could be explained by the malfunction of several tangential strain gauges during testing. The measured volumetric coefficient for granite agrees very well with the calculated value.

Table 8 Comparison between results from measurements and calculated volumetric coefficients

Coefficient of thermal expansion	Diorite	Average ($\cdot 10^{-6}$)	Granite	Average ($\cdot 10^{-6}$)
Axial, unloaded	$4 \cdot 10^{-6}$		$5 \cdot 10^{-6}$	
Axial loaded	$5 \cdot 10^{-6}$	4.5±0.5	$4 \cdot 10^{-6}$	4.5±0.5
Volumetric, unloaded	$8 \cdot 10^{-6}$		$15 \cdot 10^{-6}$	
Volumetric, loaded	$11 \cdot 10^{-6}$	9.5±1.5	$13 \cdot 10^{-6}$	14±1
Volumetric, (Equation 2) unloaded	$12 \cdot 10^{-6}$		$15 \cdot 10^{-6}$	
Volumetric, (Equation 2) loaded	$15 \cdot 10^{-6}$	13.5±1.5	$12 \cdot 10^{-6}$	13.5±1.5

One interesting difference between the diorite and the granite is that the coefficient for the loaded condition is higher than the coefficient for the unloaded condition for the diorite while the opposite is true for the granite. This is the case for both the axial and volumetric coefficient. The difference between the loading conditions is smaller for the axial coefficient than for the volumetric coefficient.
The loading compresses the sample between 20 and 100 με, but aside from this compression the shape of the expansion curves for the loaded samples look about the same as for the unloaded sample. However, the unloaded expansion curve is slightly steeper. Differences between the samples can be noted though. For most samples the hysteresis between the heating and cooling phase is smaller for the loaded condition than for the unloaded.
Sample G9 was tested under dry conditions and the resulting strains are shown in Figures 12, 13 and 14. It can be seen that the differences between the tangential and volumetric strains for the unloaded and loaded condition are small. The difference between the curves for the axial strain is about 70με, which can be attributed to the compression of the sample due to the load. The difference between the curves remains constant throughout the testing.

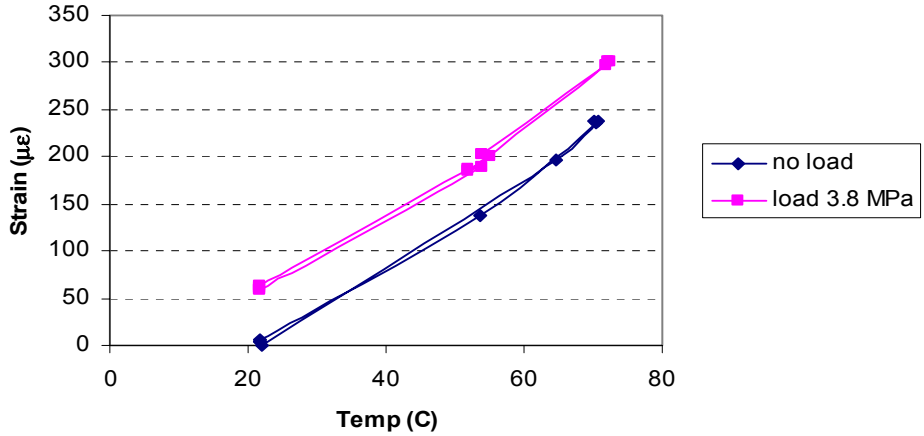

Figure 12 *Axial strain of granite sample G9 tested in air.*

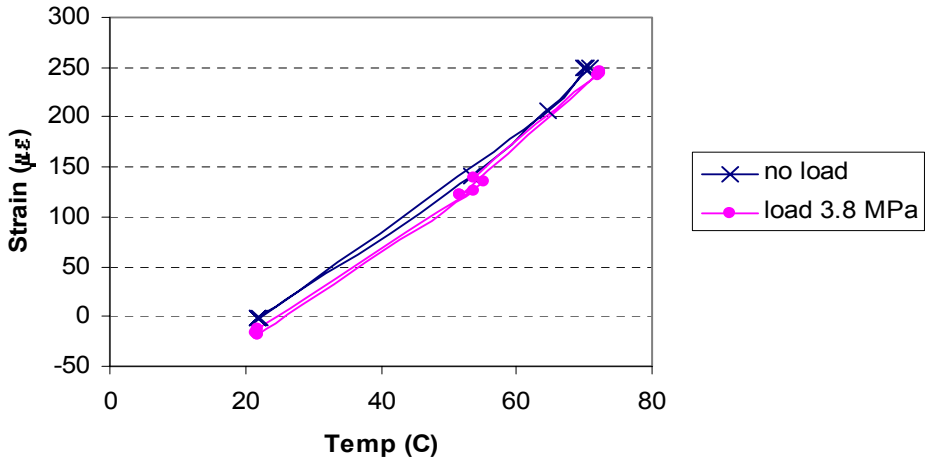

Figure 13 *Tangential strain of granite sample G9 tested in air.*

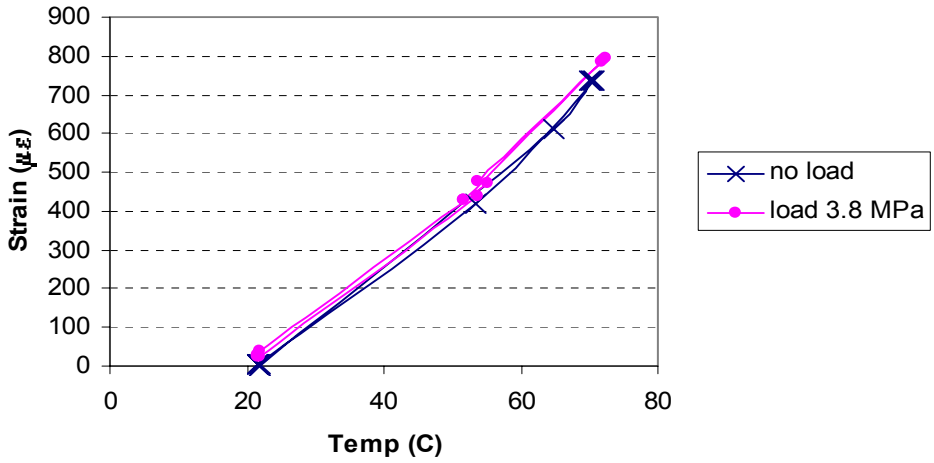

Figure 14 *Volumetric strain of granite sample G9 tested in air.*

To see if any clear differences between testing under wet or dry conditions could be found comparisons were made with sample G1. The slope of the unloaded curve is steeper than the slope of the loaded curve for the axial strain of sample G1, see Figure 5. The hystereses for the unloaded tangential and volumetric strain are larger for G1 than for G9, but the loaded and unloaded curve still follow each other closely.

It is impossible to draw any definite conclusions from this comparison, since only one sample has been tested under dry conditions. Comparing only these two samples, testing under wet or dry conditions seem to give about the same results. The fact that both the axial and volumetric coefficient is higher for sample G9 could indicate that dry conditions give larger expansion but it could also be a natural variation between the samples.

One diorite sample (D3) was also tested under dry conditions and under load but this cycle took place after the sample had been first been cycled in water so it may not be entirely representative of a dry cycle. The results from this measurement show that both the axial and volumetric coefficients of thermal expansion are higher than for the wet cycle. For this sample water already present inside the sample at the start of dry cycling could cause hydraulic cracking on a microscale when the pores are compressed during loading. This means that the difference between testing under wet or dry conditions for this sample could be temperature independent. The diagrams for sample D3 can be found in Appendix 3, page 2.

5 Discussion

5.1 Discussion

The measurements performed in this study included axial and tangential strain measured over the temperature interval from 20°C to 70°C, under two different loading conditions and under wet and dry conditions. From these measurements the axial and volumetric coefficients of thermal expansion were calculated. The measured values of the volumetric coefficient have been compared to values calculated using the simplification that the volumetric coefficient is three times the axial coefficient (Equation 2).
An average for the axial coefficient of thermal expansion is $4.5 \cdot 10^{-6}$ 1/°C and for the measured volumetric coefficient $9.5 \cdot 10^{-6}$ 1/°C for diorite and $14 \cdot 10^{-6}$ 1/°C for granite. These averages are based on the results for both loading conditions and for the axial coefficient also both rock types. The measurements indicate that the difference in axial thermal expansion between the two rock types is small for both loading conditions. For the volumetric coefficient the difference is larger. The measured volumetric coefficient corresponds well to the volumetric coefficient calculated using Equation 2, especially for granite .The value calculated by Equation 2 is $13.5 \cdot 10^{-6}$ 1/°C for both rock types. The measured coefficient for diorite deviates from the calculated values probably due to the problems with the gauges malfunctioning. The results indicate that Equation 2 gives values for the volumetric coefficient that are accurate enough, which means that if future testing is required only the axial strain needs to be measured and the axial coefficient calculated. The volumetric coefficient can then be calculated using Equation 2.
The thermal expansion of igneous rocks is influenced by for example heating rate and mineralogical composition. The effect of heating rate is that a too high rate causes microcracking even at low temperature, but with a low heating rate the microcracks can be minimized at low temperatures and will appear only when the temperature of the sample has reached the threshold value. At this threshold temperature, which is 75 – 100°C for granite(Aversa and Evangelista, 1993) the microcracks are caused by differences in thermal expansion at the grain boundaries. The more microcracks a sample contains, the higher the coefficient of thermal expansion and the higher the permanent strains. The mineralogical composition influences the thermal expansion so that the higher the quartz content the higher the thermal expansion. If a sample is homogenous (i.e. it contains only one mineral), no microcracking should theoretically occur if also the heating rate is kept low. Microcrack formation is also influenced by the surrounding pressure. If the pressure is high enough formation of microcracks can be prevented. At the depth of the prototype tunnel (450 m) the stresses are approximately:

Vertical stress: $$\sigma_v = \rho g z = 2700 \cdot 10 \cdot 450 = 12.1 MPa$$

where ρ = density (~2700 kg/m^3), g = gravity, and z = depth from the ground surface. The maximum horizontal stress can be calculated by this formula (Lundholm, 2000):

$$\sigma_H = 1.4 + 0.034 z = 16.7 MPa$$

At the tunnel boundary the major stress is then calculated as $3\sigma_H - \sigma_v$ = 38 Mpa. This suggests that the stresses are too low to prevent microcracking, since the stress required for this lies between 50 MPa and 100 MPa for granite (Ehara et al., 1983).

From the literature it can be noted that the differences in axial coefficient of thermal expansion reported by different authors can be quite large, see Table 2. The differences can in many cases be explained by the difference in temperature interval, since the thermal expansion is not linear over large temperature intervals. The measured values of the axial coefficient reported here are in fair agreement with those reported by Jumikis. Testing of the volumetric coefficient has not been found in the literature, but values of the volumetric coefficient calculated by Richter and Simmons (1974) agrees well with the values measured and calculated in this study.
To get accurate and totally reliable results more than one thermal cycle is required. In the literature it is reported that the measurements stabilized after four to five thermal cycles (Richter and Simmons, 1974) and then a residual strain is also present in the samples. A residual strain cannot be determined from the measurements reported here, since the samples were not cycled under the same conditions for more than one cycle. Microcracks in the samples may have been introduced during drilling of the boreholes and can affect the results of the measurements. This type of microcracks can be avoided if a large diameter core is chosen and then reduced to the correct dimension by using a lathe.

5.2 Sources of uncertainties and errors

Temperature measurements

The temperature of the air or water surrounding the sample was measured using a thermal element. The temperature of the sample may differ from the measured temperature, but this difference should be quite small since the water/air surrounding the sample was allowed to maintain the same temperature for a minimum of 8 hours to make sure that the temperature in the sample had reached a constant value equal to the surrounding temperature.

Strain gauges

Malfunction of strain gauges because of water entering and short-circuiting them was prevented as far as possible by adding a thick layer of silicon. The problem was to make the silicon cover the gauge and the connected wires completely. An incomplete covering was not detected immediately when the measuring started. It could take several hours before the gauge started behaving strangely and for some it was not until the cooling cycle had begun, that the strain gauge malfunctioned. This could be avoided if the samples were tested in air.
The gauges themselves measure strain very accurately, but the measuring system as a whole did have an accuracy of about 1% due to problems with keeping the temperature absolutely constant.

Grain size

The grain size adds another factor of uncertainty since different mineral types expand unequally. Depending on whether the strain gauge has been applied on a large grain or across many grains, the results differ. The strain obtained from a gauge applied on a

large grain shows only the expansion of that particular mineral. The results from a gauge across several grains are more representative for the entire sample. We placed the gauge over as many grains as possible.

Measuring equipment and technique

We decided on using a full bridge connection, which measures the average expansion over both sides of the sample. This meant that if one axial gauge failed no axial measurement data was collected after the failure. In retrospect it might have been better to measure the strain on all four gauges directly and then calculate the average. If one axial gauge failed perhaps the other continued to work and at least some data could have been collected.
The temperature measurement was not possible to include in the measurement system, so it had to be measured manually at intervals. This allows for an uncertainty since the strain varies significantly with a change in temperature of only a few degrees.

The oven

The oven is another source of error. Since the samples were to be tested under a certain load under wet conditions, the oven had to be big enough to fit both the loading device and the water container. The problem was that when the water had been heated with the immersion heater to the correct temperature and the oven door was closed the temperature of the water decreased about five degrees after which the oven started to heat the water again.

5.3 Suggestions for further work

The coefficient of thermal expansion seems to vary much within the rock type. To determine if this is just a result of coincidence, more samples would have to be tested. If more tests are decided upon, a study to determine if there are any differences between samples tested under wet or dry conditions should be made first. If dry testing gives adequate results further testing can be performed in air. It is easier to maintain an even temperature and requires less care in covering the gauges. If testing of wet samples is required, personal contact should be made with other researchers to find out exactly how they have performed their tests. Only one report by Inada and Sterling (1989) of testing of wet samples has been found within the scope of this study.
The temperature should also be measured on the face of the sample to get the correct sample temperature. The time required for leveling out the temperature gradient in the sample should also be determined. The 8 to 12 hours used in these measurements are on the safe side.
The coefficient of thermal expansion can be calculated if the mineralogical composition is known. A small attempt was made, but it was aborted due to a lack of data needed for the calculations. The lack of data was caused by the fact that not all necessary data was tabulated for all minerals, so a bit of guessing had to be done. The data in question is for example bulk modulus, density and coefficient of thermal expansion for each constituent mineral. The results were therefore not of the best quality. It would have been interesting to see how a calculated value compared to the measured values. These calculations are best performed by someone with a good knowledge of mineralogy.

6 References

AVERSA, S., EVANGELISTA, A., 1993, Thermal Expansion of Neapolitan Yellow Tuff, *Rock Mechanics and Rock Engineering* 26:4, pp 281 - 306 (ISSN: 0723-2632)

BARBISH, A. B., GARDNER, G. H. F., 1969, The Effect of Heat on Some Mechanical Properties of Igneous Rocks, *Society of Petroleum Engineers Journal* 9:4, pp 395 – 402

CLARK JR, S. P., 1966, *Handbook of Physical Constants* Revised edition. New York: The Geological Society of America Inc., pp 75 - 96 (ISBN: 99-0432009-8)

COOPER, H. W., SIMMONS, G., 1977, The Effect of Cracks on the Thermal Expansion of Rocks, *Earth and Planetary Science Letters* 36, pp 404 - 412 (ISSN: 0021-821X)

DAHLSTRÖM, L-O., 1992, *Rock Mechanical Consequences of Refrigeration: A Study Based on a Pilot Scale Rock Cavern*. Göteborg: Department of Geotechnical Engineering, Chalmers Tekniska Högskola

EHARA, S., TERADA, M., YANAGIDANI, T., 1983, Thermal Properties of Stressed Rocks, *Proceedings - Congress of the International Society for Rock Mechanics Proceedings - 5th Congress of the International Society for Rock Mechanics*, pp E137-E140

HEUZE, F. E., 1983, High-Temperature Mechanical, Physical and Thermal Properties of Granitc Rocks - A Review. *International Journal of Rock Mechanics and Mining Sciences & Geomechanics Abstract* 20:1, pp 3 - 10 (ISSN: 0148-9062)

HOMAND-ETIENNE, F., TROALEN, J-P., 1984, Behaviour of Granites and Limestones Subjected to Slow and Homogenous Temperature Changes, *Engineering Geology* 20, pp 219 - 233 (ISSN: 0013-7952)

INADA Y., STERLING, R. L., 1989, Storage of Heated Water in Underground Openings., *Journal of Geotechnical Engineering* 115:5, pp 597 - 614 (ISSN: 0733-9410)

JOHNSON, B., GANGI, A. F., HANDIN, J., 1978, Thermal Cracking of Rock Subjected to Slow Uniform Temperature Changes, *Proceedings of the 19th US Rock Mechanics Symposium May 1-3*, pp 259 - 267

JUMIKIS, A. R., 1983, *Rock Mechanics* 2nd edition. Rockport, MA: Trans Tech, s 153 - 155 (ISBN: 0-87849-038-8)

KINGERY, W.D., BOWEN, H. K., UHLMANN, D. R., 1976, *Introduction to Ceramics* 2nd edition. New York: John Wiley & Sons, pp 591 - 595 and 603 - 606 (ISBN: 0-471-47860-1)

LAMA, R. D., VUTUKURI, V. S., 1978, *Handbook on Mechanical Properties of Rocks - Testing Techniques and Results, Volume II*, Series on Rock and Soil Mechanics vol 3 (1978) no 1. Clasusthal, Tyskland: Trans Tech Publications (ISBN: 0-87849-021-3)

LOBERG, B., 1993, *Geologi 5:e upplagan*., Borås: Norstedts förlag, s 33 - 41 och 456 (ISBN: 91-1-923122-9)

LUNDHOLM, B., 2000, *Analysis of Rock Stress and Rock Stress Measurements with Application to Äspö HRL*., Luleå University of Technology, Department of Civil and Mining Engineering, Licentiate Thesis 2000:56 (ISSN: 1402-1757)

MAHMUTOGLU, Y., 1998, Mechanical Behaviour of Cyclically Heated Fine Grained Rock., *Rock Mechanics and Rock Engineering* 31:3, pp 169 - 179 (ISSN: 0723-2632)

OGAWA, T., YAMAGUCHI, U., YAMAGUCHI, K., 1994, Underground Storage of Hydrocarbons in Japan - Past and Present., *Proceedings of SPE/ISRM International Conference Eurock ´94, Rotterdam, Netherlands*: A A Balkema, pp 679 - 687 (ISBN: 90-5410-502-X)

PARK, H. D., SYNN, J. H., PARK, Y. J., KIM, H. Y., 1999, A Pilot Study on the Design of an Underground Food Storage Cavern in Korea., *Tunneling and Underground Space Technology* 14:1, pp 67 - 73 (ISSN: 0886-7798)

RICHTER, D., SIMMONS, G., 1974, Thermal Expansion Behavior of Igneous Rocks., *International Journal of Rock Mechanics and Mining Sciences & Geomechanics Abstract* 11, pp 403 - 411 (ISSN: 0148-9062)

SIMMONS, G., COOPER, H. W., 1978, Thermal Cycling Cracks in Three Igneous Rocks., *International Journal of Rock Mechanics and Mining Sciences & Geomechanics Abstract* 15, pp 145 - 148 (ISSN: 0148-9062)

SOMERTON, W. H., 1992, *Thermal Properties and Temperature Related Behaviour of Rock/Fluid Systems*. Developments in Petroleum Science 37. Amsterdam: Elsevier, pp 29 – 38 (ISBN: 0-444-89001-7)

SUNDBERG, J., 1988, *Thermal Properties of Soils and Rocks*. Swedish Geotechnical Institute, report no 35. Linköping: AB Östgöta tryck (ISSN: 0348-0755)

WALSH, J. B., 1973, Theoretical Bounds for Thermal Expansion, Specific Heat and Strain Energy Due to Internal Stress, *Journal of Geophysical Research* 78:32, pp 7637 - 7646 (ISSN:0148-0227)

VAN DEN BOGERT, P. A. J., KENTER, C. J., 1994, Computational Modelling of the Thermal and Mechanical Behaviour of Rock Mass Subjected to Cryogenic Temperatures. *Proceedings of SPE/ISRM International Conference Eurock ´94, Rotterdam, Netherlands*: A A Balkema, pp 671 - 678 (ISBN: 90-5410-502-X)

WILKINS, B. J. S., LINER, Y., RIGBY, G. L., 1985a, Time Dependent Microcracking in Plutonic Rock Due to Heat from a Nuclear Fuel Waste. *Proceedings of the 26th US Rock Mechanics Symposium, Rapid City: South Dakota* (June 1985) pp 479-486 (ISSN: 0085-574X)

WILKINS, B. J. S., LINER, Y., RIGBY, G. L., 1985b, Estimations of Changes in Microcrack-Population, Elastic Modulus and Permeability, Due to Differential-Thermal Expansion, in Plutonic Rock Surrounding a Nuclear Fuel Disposal Vault. *Materials Research Society Symposia Proceedings - Scientific Basis for Nuclear Waste Management IX Stockholm (September 1985)* pp 99-105 (ISSN: 0272-9172)

WINDOW, A. L., HOLISTER, G.S., 1982, *Strain Gauge Technology*. London: Applied Science publishers (ISBN: 0-85334-118-4)

WONG, T. F., BRACE, W. F., 1979, Thermal Expansion of Rocks: Some Measurements at High Temperatures. *Tectonophysics* 57, pp 95 - 117 (ISSN: 0040-1951)

http://www.britannica.com/bcom/eb/article/7/0,5716,63757+1+62182,00.html about quartz (2000-06-20)

http://www.britannica.com/bcom/eb/article/8/0,5716,69518+1+67759,00.html about silicate minerals (2000-06-20)

http://www.brittanica.com/bcom/eb/article/printable/9/0,5722,119049,00.html about phase changes (2000-06-20)

Other references

Chunlin Li, LTU / Boliden Mineral AB

Erling Nordlund, LTU

7 Appendices

Test 1

Date	Realtime (h.min)	Measurement time (s)	Temperature	Filename	Comments
2000-11-22	16.00	3740	19.9	Skb3	Start of measurements
2000-11-24	12.00	149310	49	Skb47	
2000-11-24	13.45	168340	50.5	Skb48	
2000-11-24	14.15	360	50.4	Skb49	
2000-11-25	12.15	77970	49.4	Skb71	Increase to 70
2000-11-26	16.45	182660	64.5	Skb99	
2000-11-27	10.35	246400	63.3	Skb118	
2000-11-27	12.50	7700	66.4	Skb120	
2000-11-27	16.30	20600	66.8	Skb124	
2000-11-28	10.30	85420	70	Skb142	
2000-11-28	11.45	90070	72	Skb143	
2000-11-28	14.20	99220	65.5	Skb146	
2000-11-28	19.15	117000	70	Skb150	The water has dissipated. Dip in The values due to opening of the oven.
2000-11-29	08.20	164220	68.1	Skb164	Decrease to 50
2000-11-29	11.40	176550	51.7	Skb167	
2000-11-29	14.45	187460	53.5	Skb170	
2000-11-29	18.00	199020	49.7	Skb173	
2000-11-30	08.20	250650	52	Skb188	Decrease to room temperature
2000-11-30	12.10	0	30.6	Skb190	
2000-12-01	08.15	72300	21.8	Skb211	
2000-12-01	12.45	88500	21.8	Skb215	
2000-12-01	14.50	96070	22	Skb217	

Samples: **D1** no load axs1 & ras1 (= channel 1 and 2)

D9 no load axs2 & ras2 (= channel 3 and 4)

Test 2

Date	Realtime (h.min)	Measurement time (s)	Temperature	Filename	Comments
2000-12-05	13.30	0	19.5	Skb218	Start 13.30
	15.55	8700	20.2	221	Increase to 50
	17.45	15340	50.4	223	
2000-12-06	08.30	68500	45.5	237	Increase to 50 again
	08.50	69480	50		
	09.25	71730	49.3	239	Gauges 2&4 vary a lot
	10.30	75600	48.8	240	
	11.40	79740	49	241	
	13.10	85060	49.4	242	Increase to 70, dip due to refill of water
	15.30	93600	70		
	18.00	102720	64.4	247	Increase to 70 again, ca 1700
2000-12-07	07.55	152660	70.1	261	
	10.35	162200	70	264	
	11.35	165950	69.9	265	Decrease to 50
	14.10	175060	57.4	267	
	15.15	179120	55.7	268	
	16.52	184850	54.1	270	
2000-12-08	08.45	242070	49.1	286	Decrease to room temperature, major dip at 242100 due to opening of the oven door
	10.35	248500	31.4		
	10.50	249660	30.2	288	
	11.55	253400	26.9	289	
	12.40	256100	25.4	290	
	16.35	0	21.3	291	
2000-12-09	10.55	66100	18.3	310	
	13.12	74150	18.1	312	

Samples: **D9** load 6.06 kN (~3.8 MPa) (channel 3 & 4)

D11 no load (channel 1 & 2)

Test 3

Date	Realtime (h.min)	Meassurement time (s)	Temperature	Filename	Comments
2000-12-11	0900	0	18.9	Skb315	Start measurement
	1105	8300	18.9	317	Increase to 50
	1205		52		
	1303	15160	48.6	319	
	1420	19900	48.3	320	
	1555	25470	49.4	322	
	1635	27930	50	323	
2000-12-12	0840	85750	53.3	339	Increase to 70
	0955		70		
	1125	95720	65.4	341	
	1535	107100	73.9	345	
	1730	117750	72.4	347	
	1915	123800	71.2	349	
2000-12-13	0715	167300	70.1	361	Decrease to 50
	0930	175130	58.8	364	
	1050	180100	56	365	
	1255	187600	52	367	
	1335	190000	51.9	368	
	1535	197100	51.9	369	
	1727	203800	51.9	372	
	2130	218500	51.8	375	Decrease to room temperature. *
2000-12-14	0830	258150	19.3	386	
	1050 ?	259400	19.6	387	

Samples: **D11** load 6.04 kN (channel 1 & 2)

D7 no load (channel 3 & 4)

Channel 3 has starting value 500 με.

* The water has dissipated so that the gauges are barely covered

Test 4

Date	Realtime (h.min)	Measurement time (s)	Temperature	Filename	Comments
2000-12-14	1530	3970	20	Skb390	
	1610	6650	20	391	
	1715	10460	20	392	Increase to 50
	1810		52		
2000-12-15	0815	64450	53.2	407	
	0935	69120	53.2	409	
	1005	71250	53.3	409	Increase to 70
	1105		70.7		
	1335	83700	65.4	413	
	1505	89150	69	414	
	1545	91450	69.8	415	
	2315	118600	70.9	422	Decrease to50
2000-12-16	1115	161850	49.4	434	
	1350	171000	49.7	437	Decrease to room temperature
	2035	195200	20.8	444	
2000-12-17		259400	18.8	461	

Samples: **D7** load 6.04 kN (channel 3 & 4)

G1 no load (channel 1 & 2)

Channel 3 has start value 300 με.

Test 5

Date	Realtime (h.min)	Measurement time (s)	Temperature	Filename	Comments
2000-12-17	1710	340	20	Skb463	
	1815	4400	20	463	Increase to 50
	1910		51.7		
2000-12-18	0835	55950	49.6	477	
	0935	59450	49.5	478	
	1010	61550	49.6	479	Increase to 70
	1115		70.6		
	1245	71000	66.8	482	
	1500	79000	72.7	484	
	1620	83900	74.3	485	
	1820	91100	72.4	487	
	2255	103800	71.3	492	Decrease to 50
2000-12-19	0810	140750	49.7	501	
	1020	148600	49.5	503	
	1215	155600	49.4	505	Decrease to room temperature
	1350		34		
	1515		28		
	2040	185850	20.5	514	
2000-12-20	0815	227300	18.5	525	

Samples: **G1** load 6.06 kN (channel 1 & 2)

G5 no load (channel 3 & 4)

Test 6

Date	Realtime (h.min)	Measurement time (s)	Temperature	Filename	Comments
2001-01-04	1630	0	22.5	Skb 527	
	1710	2560	22	528	Increase to 50
2001-01-05	1000	63350	64.7	545?	Increase to 70
	1145		71.1		
	1230	72250	70.4	548	
	1915	96400	70.1	554	
2001-01-06	1240	159100	70.8	571	Decrease to 50
	~14		61.8		
	1450		61.3		
	1530		59.1		
2001-01-07	1510	255700	53.5	598	Decrease to room temperature
2001-01-08	0815	0	21.7	601	
	1100	10000	21.7	603	
	1220	14800	21.8	604	

Samples: **G9** no load (channel 1 & 2)

Note! This sample is tested in air.

Start value, channel 1: 200 με.

Test 7

Date	Realtime (h.min)	Measurement time (s)	Temperature	Filename	Comments
2001-01-08	1600	830	21.7	Skb 607	
	1815	9350	21.8	608	Increase to 50
2001-01-09	0845	61800	53.8	623?	
	0950	65600	51.8	624	
	1110	70300	51.8	625	Increase to 70
	1240		69.2		
	1330		70.9		
	1425		72.7		
	1550	87200	71.9	630	
	1630		72.3		
	1740	93750	72.2	632	
2001-01-10	0840	147800	72.4	647	Ca 0930 decrease to 50
	1100		61.3		
	1630		53.7		
	1810		53.8	656	
2001-01-11	0815	232700	55.2	670	Decrease to room temperature
	1015		28		
	1100		24		
	1320		22.4		
	1700	0	21.8	678	
2001-01-12	0830	55500	21.6	694	
	0915				

Sample: **G9** load 6.06 kN (channel 1 & 2)

Note! This sample is tested in air.

Start value, channel 1: 200 με.

Test 8

Date	Realtime (h.min)	Measurement time (s)	Temperature	Filename	Comments
2001-01-12	1045	0	21.2	Skb697	
	1155	4250	20.5	698	
	1250	7450	20.2	699	
	1345	10900	19.9	700	
	1410				Increase to 50
	1500		50.7		
	1535		48.5		
	1715	23300	49	703	
2001-01-14	1215	178300	56.4	746	Increase to 70
	1300		70		
	1345		65.7		
	1940	204900	70.3	754	
2001-01-15	0830	250900	70.4	766	Decrease to 50, axial gauge down
	1015		59.5		
	1120		56.5		
	1515	14000	52.5	773	
	1610	17370	52	774	
	1815	24900	51.4	776	
2001-01-16	0845	76950	50.5	790	Decrease to room temperature
	1530	101350	21.3	797	
	1745	109450	20.3	800	
2001-01-17	0830	162300	18.7	814*	Both gauges down

* Choose a file from the night when the tangential gauge is still working. Temperature is assumed to be the same as at 0830.

jkhkjh

Sample: **G5** load 6.14 kN (channel 3 & 4)

Test 9

Date	Realtime (h.min)	Measurement time (s)	Temperature	Filename	Comments
2001-01-17	0915	1050	21.3	Skb817	
	1120	8450	20.7	818	Increase to 50
	1210		49.5		
	1330		46.5		
	1530	23450	47.1	822	
	1710	29600	48.2	824	
2001-01-18	0815	83700	53	839	Increase to 70
	0900		70		
	1000		65		
	1245	100000	67.3	844	
	1440	106800	69	846	
	1550	111200	69.1	847	
2001-01-19	0830	171300	66.6	863	Decrease to 50
	1010		55.7		
	1145		53.4		
	1305	187500	51.6	868	
	1410	191650	50.8	869	
	1545	197250	50.4	871	
2001-01-20	0955	0	54.2	888	Decrease to room temperature
2001-01-22	0835	168100	19.7	935	
	0930	171500	19.5	936	

Sample: **D5** load 6.06 kN (channel 1 & 2)

Test 10

Date	Realtime (h.min)	Measurement time (s)	Temperature	Filename	Comments
2001-01-22	1120	1120	20.2	Skb939	
	1340	9500	19.7	941	
	1510	14900	19.5	942	
	1615	18500	19.6	943	Increase to 50
	1705		50.2		
2001-01-23	0815	76300	49.1	959	
	0935	81050	49.4	960	
	1025	84150	49.6	961	Increase to 70
	1125		70.6		
	1250		65.5		
	1330		66.2		
	1505		68.2		
	1525		68.7		
	1700	107800	70.4	968	
2001-01-24	0900	165500	69.4	984	Decrease to 50
	1135		55.7		
	1340	182150	51.4	989	
	1400		51		
	1505	187150	50	990	
2001-01-25	0855	251450	49.9	1008	Decrease to room temperature
	1010		38		
	1305	100	26.1		
	1510	7600	23		
2001-01-26	0825	69800	18.8	1030	
	1015	76300	18.7	1032	
	1050	78200	18.7	1033	

Sample: **D3** load 6.06 kN (channel 3 & 4)

Start value: axs2 400με without load

axs2 353με with load

ras2 20με with load

Stop value: axs2 369με with load

ras2 70με with load

axs2 427με immediately after unloading

ras2 60με immediately after unloading

axs2 417με 20 min after unloading

ras2 54με 20 min after unloading

Test 11

Date	Realtime (h.min)	Measurement time (s)	Temperature	Filename	Comments
2001-01-26	1130	0	20.7	Skb1035	
	1500	12400	19.7	1038	Increase to 50
	1545		50		
	1730		46.1		
2001-01-27	1605	102900	48.7	1063	Increase to 70
	1650		68.1		
2001-01-28	1310	178850	70.7	1084	Decrease to 50, tangential gauge down
2001-01-29	0900	250100	52.2	1104	
	1010	254150	52.5	1105	Increase to room temperature
	1345		29.7		
	1715		22.6		
2001-01-30	0845	72850	18.5	1128	
	1015	77700	18.5	1129	

Sample: **D1** load 6.06 kN (channel 3 & 4)

	Without load		with load	
Start value	axs1	400 με	430 με	
		Ras1	0 με	-54 με

Test 12

Date	Realtime (h.min)	Measurement time (s)	Temperature	Filename	Comments
2001-01-30	1530	1100	22.4	Skb1131	
	1645	5150	22.2	1132	1730 Increase to 50
2001-01-31	0830	62050	58.1	1148	
	1015	68150	58.2	1149	Increase to 70
	1120		71		
	1255	77150	71.8	1152	
	1405	81950	72.2	1153	
	1650	91750	69.6	1156	
2001-02-01	0855	149750	68.7	1172	Decrease to 50
	1005		59.7		
	1225		57.5		
	1315		46.9		
	1340		48.3		
	1510		46.6	1178	
	1650		45.9	1180	
2001-02-02	0835		44.5	1195	Decrease to room temperature
	0940		33.4		
	1105		28.6		
	1255		23.7		
	1510	258750	22.9	1203	
	1715	7400	22.5	1205	
2001-02-03	1530	87900	21.7	1227	Unloading
2001-02-04	1230	163050	20.8	1248	

Sample: **D3** load 6.06 kN (channel 3 & 4) Tested in <u>air</u>

		Without load		with load	
Start value	axs2	400 με		351 με	
		Ras2	0 με		16 με

In these files axs1 denotes axial strain for sample 1, ras 1 = tangential strain for sample 1, axs 2= axial strain for sample 2 and ras 2 = tangential strain for sample 2.

When the standard deviation calculated from the average values of the strain in the measurement files produced was larger than 3, they were marked with *. This was done so that if the average value for that temperature deviated largely from the drawn curve it could be excluded from the following calculations. When the sample had been kept at a constant temperature for about 8 hours the standard deviation was usually quite low, but if the strain gauges started to malfunction during that time the value did not stabilize but could instead increase alarmingly.

Test 1

Temp	Load	Axs1	Ras1	Axs2	Ras2
19.9	1.980219	12.71118	11.15834	17.45668	13.84332
50.5	1.935238	-102.1484	-92.74028	-95.02875	-44.69874
50.4	1.93485	-102.2852	-91.2274	-93.97545	-43.80134
49.4	1.936564	-85.0213	-60.50171	-84.34652	-21.00206
64.5	1.910619	-111.5153	-69.87413	-103.6798	-97.06042
63.3	1.904383	-107.0136	-59.34098	-91.46109	-2.678848
66.4	1.901507	-113.3613	-65.31739	-95.57834	-18.94149
66.8	1.897965	-115.0906	-65.71289	-96.16292	15.55056
70.0	1.890082	-129.3077	-72.8003	-107.982	25.43528
72.0	1.890449	-129.7499	-73.89418	-107.7013	30.74884
65.5	1.894644	-116.5636	-62.43232	-94.34271	41.65175
70.0					
68.1	1.891312	-132.3378	-98.33984	-105.0252	-1.157526
51.7	1.905906	-84.35683	-47.8087	-57.70969	23.14223
53.5	1.91161	-81.97822	-44.22594	-54.54251	25.28877
49.7	1.913896	-77.63374	-38.93392	-50.59313	27.41943
52.0	1.915282	-77.4962	-35.73663	-48.77197	26.18856
30.6	1.924816	-31.27432	14.01445	-5.389569	49.7861
21.8	1.9632	23.13653	76.38998	44.19542	78.94898
21.8	1.962753	21.58176	76.79701	43.30553	80.29745
22.0	1.961395	19.20851	73.98687	40.75651	78.91374
		D1	D1	D9	D9

Test 2

Temp	Load	Axs1	Ras1	Axs2	Ras2
20.2	6.029106	13.99875	6.534531	-39.30827	14.19135
50.4	5.985489	-86.53659	-44.59616	-143.6741	-52.30442
45.5	5.93443	-69.51891	49.79262	-121.3284	-32.13718
49.3	5.926936	-88.12921	45.02787	-137.679	8.765733
48.8	5.925049	-82.83081	57.57162	-132.4164	-22.63306
49.0	5.923212	-83.22808	60.00489	-132.4178	-25.77243
49.4	5.92121	-84.31478	61.942	-133.3455	-38.7797
64.4	5.890736	-170.6489	46.85581	-220.8266	-68.84766
70.1	5.793366	-160.1793	163.8658	-216.98	6.361194
70.0	5.777307	-154.8543	176.2356	-211.1477	16.59628
69.9	5.774073	-158.4798	149.3187	-212.5176	18.99043
57.4	5.800156	-124.0953	107.2171	-206.3924	38.18739
55.7	5.807162	-110.7503	78.76017	-198.7237	46.70533
54.1	5.812604	-97.87327	118.5357	-194.6248	56.17554
49.1	5.829595	-66.7117	14.57883	-145.6448	75.26286
30.2	5.876886	-12.55023	-39.07756	-84.07525	75.82384
26.9	5.886748	4.042186	-8.937144	-67.01036	89.80347
25.4	5.892191	14.25944	3.261356	-56.86863	95.4522
21.3	5.897315	20.23581	12.07631	-51.28068	98.24537
18.3	5.910219	57.3759	102.5784	-23.77279	126.7117
18.1	5.91092	59.14687	102.771	-23.3568	132.9264
		D11	D11	D9 loaded	D9 loaded

Test 3

temp	load	axs1	ras1	ras2	axs2	st dev > 3
18.9	4.449963	-37.21503	9.824246	2.091029	1.47203	
18.9	6.024041	-56.4171	4.993984	-0.296439	-0.585962	
48.6	5.958142	-189.2836	-60.94266	-113.3721	-106.6528	*
48.3	5.948226	-173.6084	-18.33135	-92.14858	-90.27506	
49.4	5.940088	-171.4803	8.760018	-85.28008	-86.655	
50	5.93583	-174.943	12.994	-87.70101	-89.69726	
53.3	5.922724	-190.4216	16.32107	-70.87837	-93.7717	
65.4	5.901733	-253.1155	13.07554	-105.4647	-145.3084	*
73.9	5.825757	-263.9486	110.3236	-91.08521	-146.011	*
72.4	5.811311	-267.1712	83.18047	-91.30249	-147.5694	
71.2	5.804844	-260.3936	84.81527	-82.66141	-141.6029	
70.1	5.776983	-248.8634	104.4162	-52.97065	-130.6573	
58.8	5.805922	-206.7518	51.52493	-24.6323	-92.62831	*
56	5.811688	-194.3441	57.44738	-13.79924	-81.02891	
52	5.824032	-177.7751	52.98896	0.4309533	-65.03499	
51.9	5.826082	-172.8855	60.06619	5.791179	-60.38277	
51.9	5.824679	-172.7797	61.23915	6.605865	-60.24713	
51.9	5.825813	-172.6332	62.68528	8.671999	-59.64083	
51.8	5.824409	-172.3389	64.04148	10.7202	-58.63036	
19.3	5.906214	-50.96124	48.79069	114.2971	50.29029	
19.6	5.907132	-50.43529	50.3493	115.611	51.49949	
		D11 loaded	D11 loaded	D7	D7	

Test 4

temp	load	axs1	axs2	ras2	axs2	st dev > 3
20	5.98559	-0.2312	3.729789	18.40535	142.9647	
20	5.984887	-0.240907	4.211551	18.7519	143.0135	
53.2	5.894077	-130.4864	-132.6525	-113.9608	19.40918	*
53.2	5.892245	-128.5265	-130.2951	-92.78836	19.3495	
65.4	5.85053	-165.3361	-161.24	-117.7829	-25.35129	
69	5.839882	-171.0056	-166.2679	-121.2335	-32.82199	*
69.8	5.830353	-183.0878	-179.0853	-134.0725	-47.71999	*
70.9	5.823652	-184.5771	-173.3588	-143.7975	-58.75245	
49.4	5.872359	-98.75353	-77.70711	-65.9611	37.0497	*
49.7	5.872143	-99.75723	-75.0194	-68.27895	35.44786	*
20.8	5.942999	0.0205925	47.36423	31.99219	141.489	
18.8	5.94758	5.918225	57.66656	20.8436	151.5083	
		G1	G1	D7 loaded	D7 loaded	

Test 5

temp	load	axs1	ras1	axs2	ras2	st dev > 3=*
20	6.127291	-58.0508	9.562889	1.066231	1.412449	
49.6	6.040153	-155.9801	-105.032	-187.7021	-139.4558	
49.5	6.039669	-155.6193	-104.6251	-185.1508	-136.6333	
49.6	6.040693	-155.0252	-104.2901	-180.6464	-134.3967	
66.8	5.992089	-201.5313	-164.0069	-189.525	-172.1544	*
72.7	5.948603	-212.7672	-179.0107	-207.468	-179.7865	*
74.3	5.936047	-225.7745	-193.6645	-224.703	-191.4537	*
72.4	5.9191	-226.0268	-192.2648	-235.0993	-185.4235	*
71.3	5.913036	-222.3863	-177.5838	-191.7833	-158.2574	*
49.7	5.962454	-149.0289	-86.95909	-106.8983	-62.92996	
49.5	5.961483	-145.9432	-87.44426	-101.0267	-62.44304	*
49.4	5.961645	-143.9006	-84.19135	-97.24394	-81.86076	
20.5	6.034495	-54.11635	21.52398	31.3227	62.24311	
18.5	6.037243	-46.12902	20.43851	41.53103	75.14852	
		G1 loaded	G1 loaded	G5	G5	

Test 6

temp	load	ras1	axs1	korr axs1	st dev >3
22	0	0.336478	198.4816	-1.5184	
64.7	0	-169.093	39.4847	-160.515	
70.4	0	-202.61	9.5822	-190.418	
70.1	0	-204.037	8.0543	-191.946	
70.8	0	-201.923	8.7781	-191.222	
53.5	0	-120.5	82.5377	-117.462	
21.7	0	0.27573	193.9377	-6.06233	
21.7	0	0.529116	194.5679	-5.43215	
21.8	0	0.109516	194.6628	-5.3372	
		G9	G9		

Test 7

temp	**load**	**axs1**	**ras1**	**korr axs1**	**st dev >3**
21.7	6.03983	140.60058	16.96425	-59.39942	
21.8	6.037728	140.41205	17.06394	-59.58795	
53.8	5.94052	31.4385	-104.8503	-168.5615	
51.8	5.940682	31.3954	-104.9493	-168.6046	
51.8	5.941274	31.9803	-104.7146	-168.0197	
71.9	5.891652	-48.5168	-193.613	-248.5168	
72.2	5.887556	-50.8755	-195.303	-250.8755	
72.4	5.885347	-51.5078	-195.6407	-251.5078	
53.8	5.922185	17.8059	-118.0732	-182.1941	
55.2	5.923375	21.2397	-113.1171	-178.7603	
21.8	5.999518	136.09005	12.23246	-63.90995	
21.6	6.001831	138.47658	15.88515	-61.52342	
		G9 loaded	G9 loaded		

Test 8

temp	load	axs2	ras2	st dev > 3
21.2	6.101018	-61.38501	19.13848	
20.5	6.100447	-60.19816	18.91561	
20.2	6.101848	-58.02735	18.90015	
19.9	6.104273	-56.32582	18.77333	
49	6.037782	-150.5412	-89.01639	
56.4	5.989326	-162.439	-61.67874	
70.3	5.92559	-207.27	-106.7044	
70.4	5.902971	-186.187	-100.7012	axs 2 = st dev 9
52.5	5.928825	-379.1797	-25.57156	axs 2, st dev = 259
52	5.929039		-22.18533	
51.4	5.930925		-17.23199	
50.5	5.931628		-7.224895	
21.3	6.005015		108.6806	
20.3	6.01019		117.8413	
18.7	6.013424		120.7361	not the right temperature, taking file no 803
		G5 loaded	G5 loaded	

Test 9

temp	load	axs1	axs2	st dev > 3
21.3	6.137851	-45.64087	13.99014	*
20.7	6.135046	-42.61841	15.64439	
47.1	6.058802	-125.746	-42.19496	
48.2	6.051309	-131.6447	-46.5705	
53	6.03374	-161.6306	-58.25304	c*
67.3	5.961268	-203.5848	-75.91268	
69	5.943322	-215.9085	-80.03472	
69.1	5.942352	-218.6876	-80.46902	
66.6	5.938095	-207.5629	-53.60121	
51.6	5.976736	-151.18	-16.97795	
50.8	5.978998	-147.4067	-14.21807	
50.4	5.98121	-140.6969	-10.75745	
54.2	5.975333	-158.728	-17.63753	
19.7	6.059072	-39.45218	63.94708	
19.5	6.059342	-38.93731	64.43522	
		D5 loaded	D5 loaded	

Test 10

temp	load	ras2	axs2	st dev >3
20.2	6.088562	24.94275	-41.3448	
19.7	6.085303	24.44797	-39.97529	
19.5	6.086166	24.80523	-39.44905	
19.6	6.085033	25.59137	-38.32737	
49.1	6.001671	-112.58	-153.7462	
49.4	6.001076	-113.0683	-154.8041	
49.6	6.000103	-113.3789	-155.4009	
70.4	5.884107	-198.8159	-242.6365	
69.4	5.867132	-174.9159	-239.5114	
51.4	5.919857	-90.36255	-166.4415	
50	5.921318	-83.68639	-160.7381	
49.9	5.922618	-73.45513	-155.2341	
18.8	6.004421	64.45955	-34.14712	ras
18.7	6.004099	69.89136	-32.83691	
18.7	6.003867	70.26637	-32.05817	
		D3 loaded	D3 loaded	In water

Test 11

temp	load	axs1	ras1	korr axs1
20.7	6.052178	433.97541	-51.4104	33.97541
19.7	6.051859	439.68504	-48.26023	39.68504
48.7	5.966284	309.63949	-110.3665	-90.36051
70.7	5.847004	192.6988		-207.3012
52.2	5.899052	289.9929		-110.0071
52.5	5.899642	290.5843		-109.4157
18.5	5.985718	463.89433	193.2671	63.89433
18.5	5.984097	464.85599	181.505	64.85599
		D1 loaded	D1 loaded	

Test 12

temp	load	axs	korr axs	ras	st dev > 3
22.4	6.063454	349.68061	-50.31939	15.73079	
22.2	6.062916	349.56735	-50.43265	15.88162	
58.1	5.964501	190.5518	-209.4482	-177.4672	
58.2	5.964447	191.1811	-208.8189	-177.0033	
71.8	5.93664	132.902	-267.098	-245.1579	
72.2	5.933513	129.3959	-270.6041	-249.2838	
69.6	5.93443	140.8379	-259.1621	-238.7478	
68.7	5.935669	143.1396	-256.8604	-241.2638	
46.6	5.979815	239.6417	-160.3583	-132.9902	ras, axs
45.9	5.988031	250.7243	-149.2757	-120.3532	
44.5	5.993168	255.7766	-144.2234	-113.8102	
22.9	6.039905	340.25691	-59.74309	-11.04192	
22.5	6.04204	343.11928	-56.88072	-8.108644	
21.7	6.047106	345.9893	-54.0107	-4.009078	
20.8	-0.133268	399.01939	-0.980609	-18.03644	
		D3 loaded	D3 loaded		In air

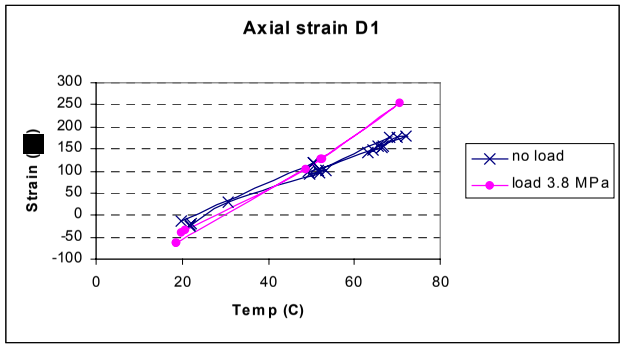
Axial strain D1
Strain (με)
Temp (C)
no load
load 3.8 MPa

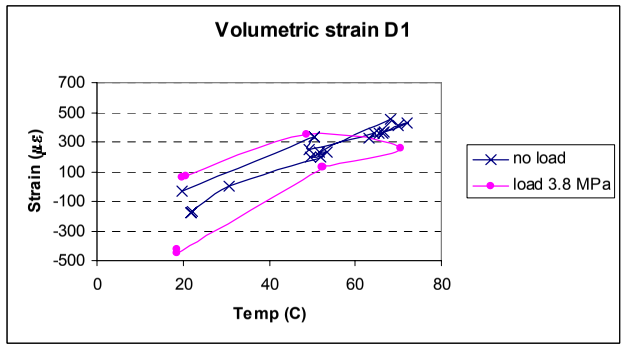
Volumetric strain D1
Strain (με)
Temp (C)
no load
load 3.8 MPa

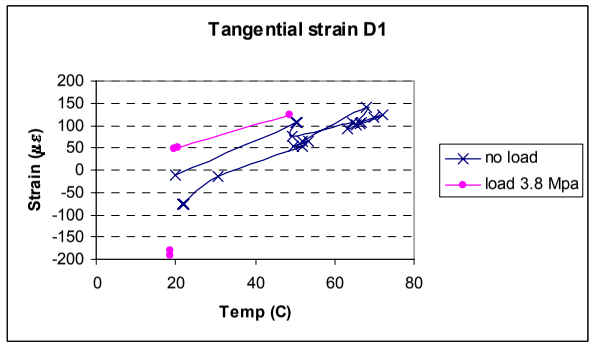
Tangential strain D1
Strain (με)
Temp (C)
no load
load 3.8 Mpa

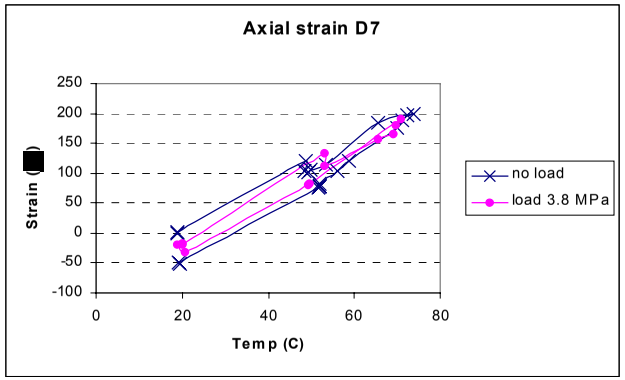
Axial strain D7
Strain (με)
Temp (C)
no load
load 3.8 MPa

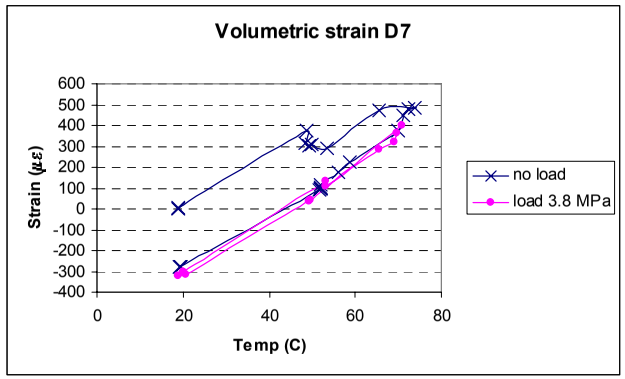
Volumetric strain D7
Strain (με)
Temp (C)
no load
load 3.8 MPa

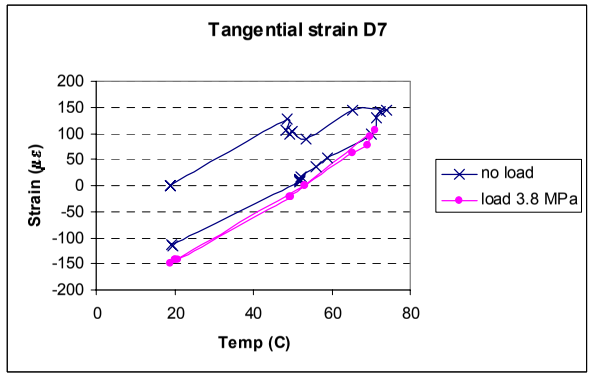
Tangential strain D7
Strain (με)
Temp (C)
no load
load 3.8 MPa

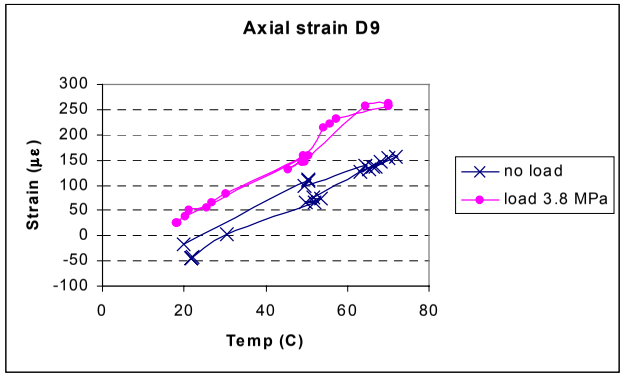
Axial strain D9
Strain (με)
Temp (C)
no load
load 3.8 MPa

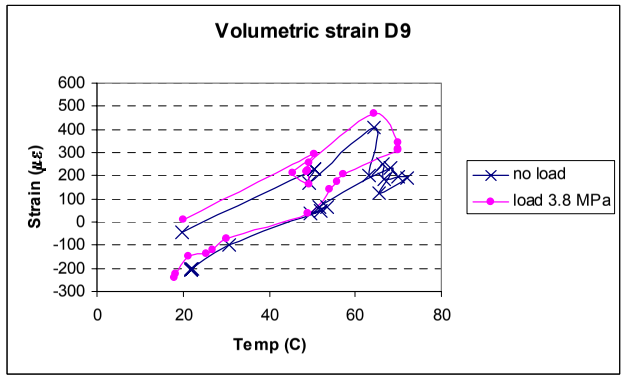
Volumetric strain D9
Strain (με)
Temp (C)
no load
load 3.8 MPa

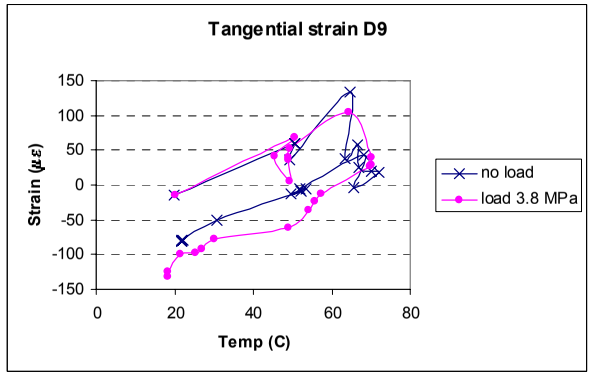
Tangential strain D9
Strain (με)
Temp (C)
no load
load 3.8 MPa

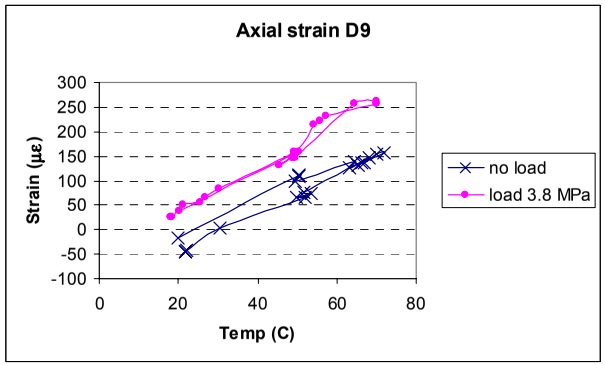
Axial strain D9
Strain (με)
Temp (C)
no load
load 3.8 MPa

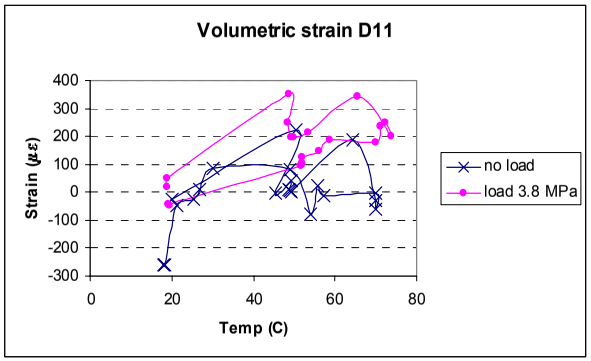
Volumetric strain D11
Strain (με)
Temp (C)
no load
load 3.8 MPa

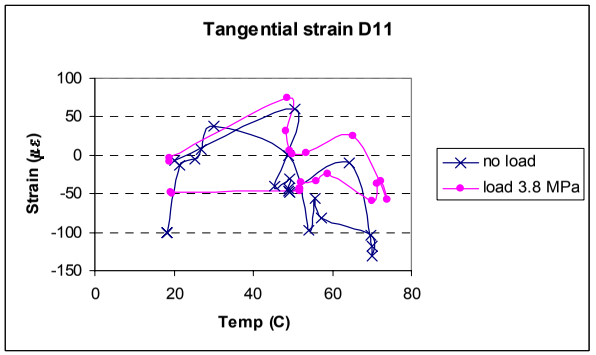
Tangential strain D11
Strain (με)
Temp (C)
no load
load 3.8 MPa

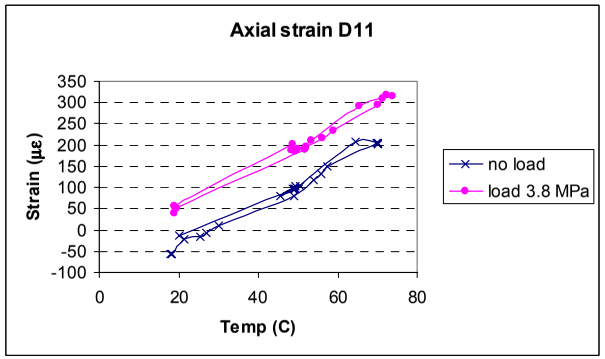
Axial strain D11
Strain (με)
Temp (C)
no load
load 3.8 MPa

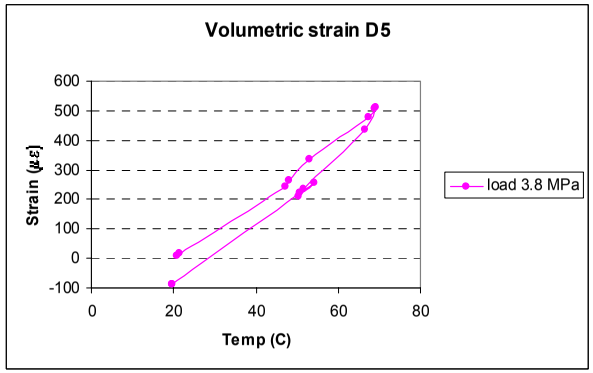
Volumetric strain D5
Strain (με)
Temp (C)
load 3.8 MPa

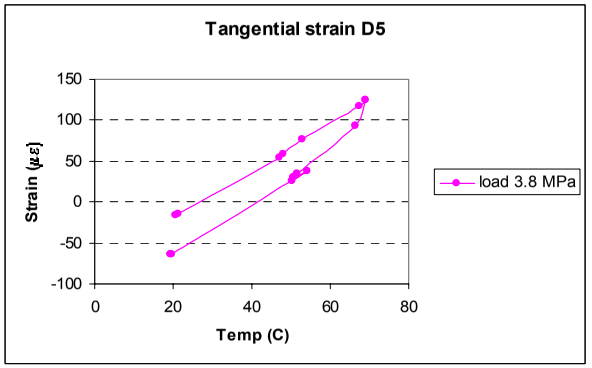
Tangential strain D5
Strain (με)
Temp (C)
load 3.8 MPa

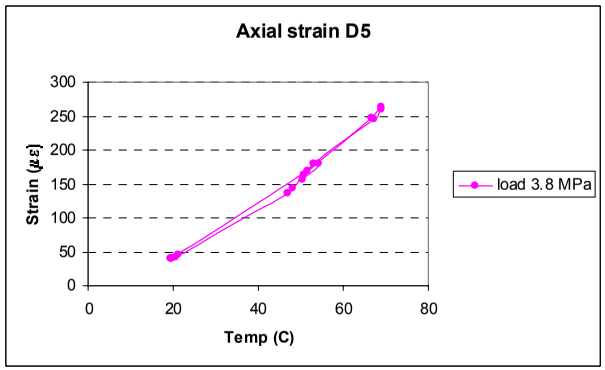
Axial strain D5
Strain (με)
Temp (C)
load 3.8 MPa

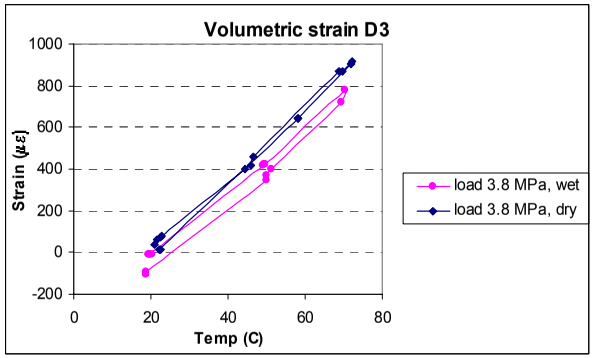
Volumetric strain D3
Strain (με)
Temp (C)
load 3.8 MPa, wet
load 3.8 MPa, dry

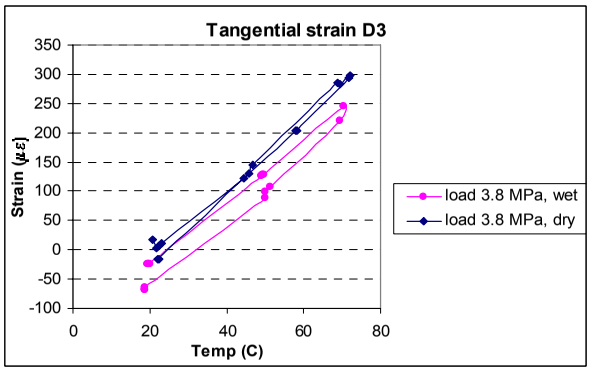
Tangential strain D3
Strain (με)
Temp (C)
load 3.8 MPa, wet
load 3.8 MPa, dry

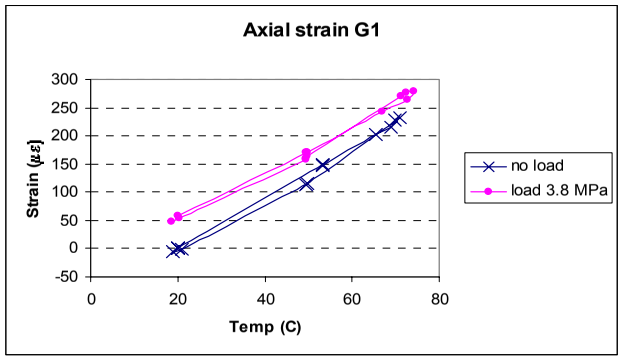
Axial strain G1
Strain (με)
Temp (C)
no load
load 3.8 MPa

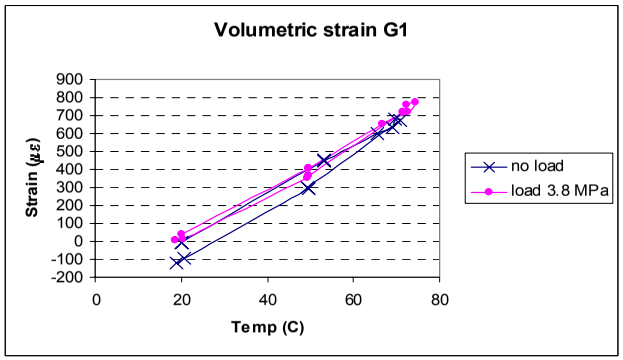
Volumetric strain G1
Strain (με)
Temp (C)
no load
load 3.8 MPa

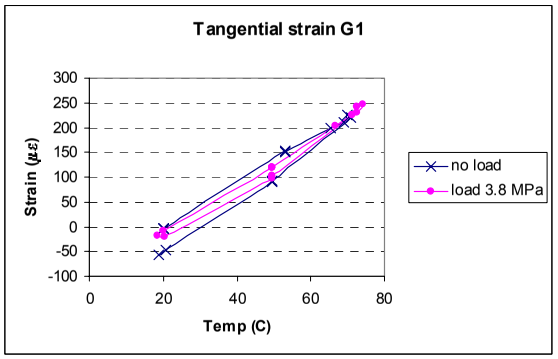
Tangential strain G1
Strain (με)
Temp (C)
no load
load 3.8 MPa

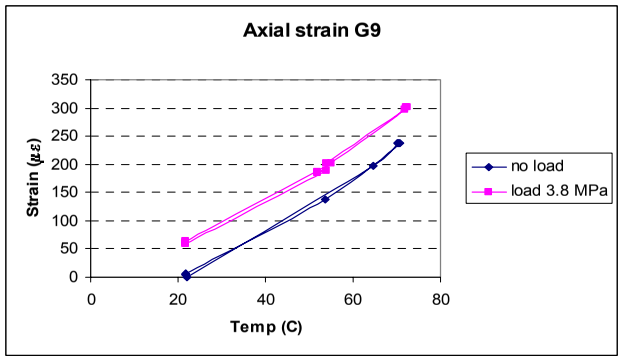
Axial strain G9
Strain (με)
Temp (C)
no load
load 3.8 MPa

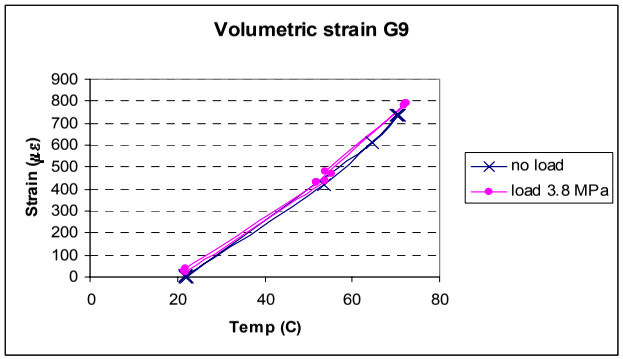
Volumetric strain G9
Strain (με)
Temp (C)
no load
load 3.8 MPa

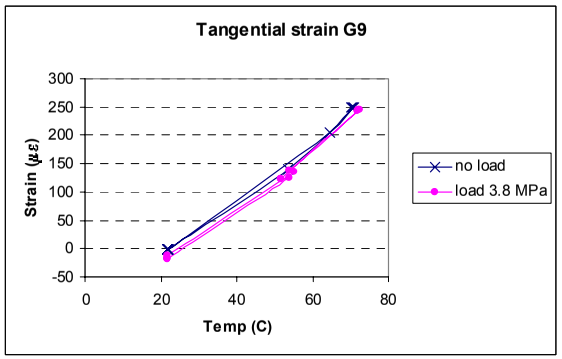
Tangential strain G9
Strain (με)
Temp (C)
no load
load 3.8 MPa

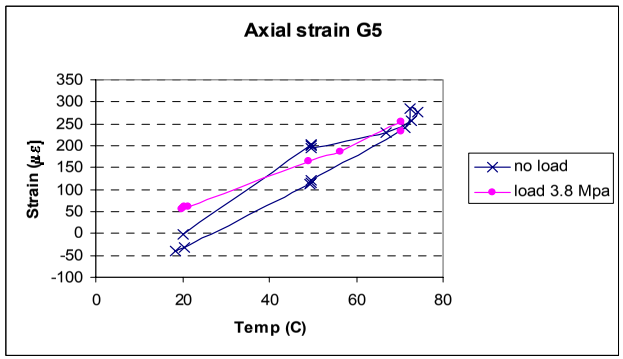
Axial strain G5
Strain (με)
Temp (C)
no load
load 3.8 Mpa

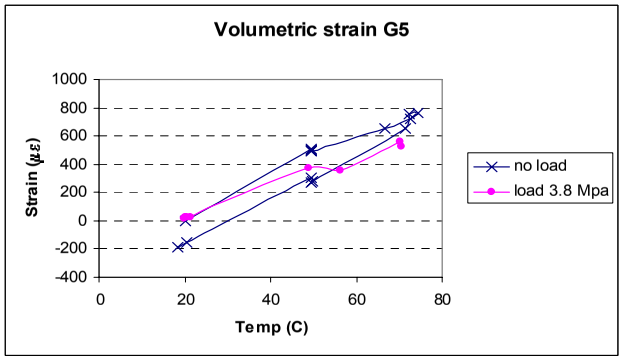
Volumetric strain G5
Strain (με)
Temp (C)
no load
load 3.8 Mpa

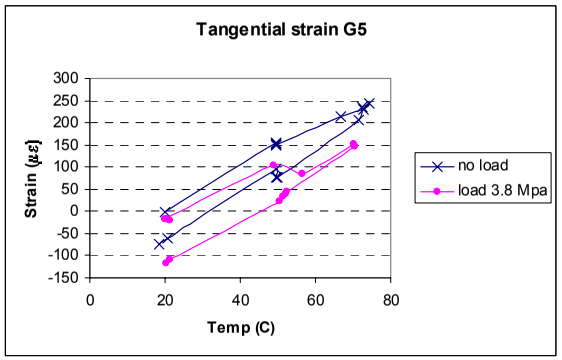
Tangential strain G5
Strain (με)
Temp (C)
no load
load 3.8 Mpa